

Revision Guide

1. Point-by-point reply to the comment

The comments will be repeated in black, as our responses will be noted in red, referring to the manuscript with the highlighted changes attached to this guide.

a. Referee 1

[...]

I have three main concerns:

(1) Whereas the approach is useful as mentioned above, I am missing information on its novelty. Has anybody done this before? If not, why not outlining clearly that this is a novel approach. The introduction references studies by Anderson and Steenpass but differences and similarities to the present study remain unclear.

As of our knowledge, neither in thermal remote sensing nor in catchment hydrology where the delineation of hydrological response units or functional units including their parameterization is subject to research is there any publication on the use of complex time series analysis of TIR data in combination with PCA as used here. In this sense, our approach is new. However, we recently got aware of the application of empirical orthogonal functions (EOF) that seem to be frequently used in oceanography and atmospheric research (e.g. Denbo & Allen, 1984; Hamlington et al., 2011; Lorenz, 1956). The approach is similar to PCA with an adjustment considering the extent of a single spatial data point/model output due to calculations on a global coordinate system and therefore occurring contortions. Nevertheless, the used data and the suggested applications differ largely.

We noted in which way our approach is a novelty within the abstract (p1, l19), as well as extended the rationale in the PCA section (p8, l25-30).

Anderson et al. (2011) and Steenpass et al. (2010) are both using similar thermal RS data within their work. However, Anderson et al. focus on the translation of thermal data into evapotranspiration data and, therefore, are limited to real data transformation based on the knowledge of physical processes. Steenpass et al. use the data to derive hydrological properties by the use of inversion. These two approaches differ largely from ours. They are mainly quoted to note **different** appliances of TIR data, as noted.

We removed the example from Anderson et al. and clarified the approach from Steenpass et al. (p3, l20-22).

(2) The methods appear rather complicated, except for the PCA which is well established and applicable in this context. Are the other methods also established or are they applied for the first time here? I do not understand why and how these methods were chosen. Further, I do not understand the benefit of investigating the

persistence; and the added value of the behavioral measure analysis over the PCA.

Our main intention using all of the presented methods is to strengthen the reliability of our results. The first part on “persistence measures” is to our knowledge novel and our own contribution in terms of a new methodology of spatial data exploration. By applying these persistence methods we are able to confirm the existence of spatially and temporally consistent patterns within the time series of images. This finding supports the application of a principle component analysis (PCA) where the most dominant patterns (in the form of independent principle components) within the time series are extracted and information on explained variance by that PC is given.

It could be argued, that a PCA resulting in PCs with a significant high percentage of explained variance would be sufficient to confirm pattern persistency. However, there might be situation where 2 (or more) PCs with a high percentage of explained variance exist, but where e.g. some oscillating landscape behavior might result in non-persistent time series.

We added an appropriate part to the persistency section (p6, l21-26).

The part on behavioral measure analysis is a new approach to classify the dataset into functional units (or hydrological response units, here only under radiation driven condition, see Zehe et al. 2014 for an extended discussion). We assume that different loading values derived from PCA are related to a dominance of a different PC and therefore a different control on land surface temperature (LST) (and hence related to the functioning of the land and sub-surface as a reaction to the differing meteorological short time history and surface states). In this way we can choose a limited set of LST-images showing most distinct patterns. The derived classification by using the 5 most distinct LST-images is a representation of the spatio-temporal dynamics of LST and therefore of the “real landscape functioning”. We are currently not in the situation to evaluate this procedure as superior to other classification methods (e.g. using the first 5 PCs, deviding them into a number of classes and intersecting them). Such an approach would involve a catchment scale hydro-meteorological modelling exercise, where different classification methods are compared with regard to effectiveness of parameterization and the quality of modelling results. While this is beyond the scope of this paper, it is motivation for current research and we will briefly add that in the outlook part of the paper.

Overall, we belief that the persistency analysis is a very helpful additional tool needed to avoid biased handling of the dataset. The behavioral measure is used to complete the PCA to spatially classify the catchment concerning the compartments' functioning.

We tried to clarify the part on behavioural measures by rearranging parts (p 11, l7-20). An evaluation is not a part of this paper.

(3) Please improve the English language throughout the manuscript. I have seen worse papers, but some improvements would facilitate the readability and clarify the message in some places.

We had a native speaker for examination of the quality of the text for the initial version as well as a second expert for the revised version. Minor changes were made throughout the text.

Title

Is "catchment functional unit" an established term? I would suggest to use hydrological response unit.

We do not change the title on purpose – because we like the expression functional units and it is consistent with our project's nomenclature.

Abstract

line 8: what is ASTER? We explained the abbreviation in the abstract and the introduction.

line 9: change "The application mathematical-statistical" to "The application of mathematical-statistical" Changed.

line 14: "binary word" is not introduced before and hard to understand Clarified.

page 7021:

lines 22/23: also phenology and leaf area index may be impacted by hydrology, for example in dry regions. Deleted.

page 7022:

line 1: change "atmospheric states" to "atmospheric state" Changed.

lines 10/11: please elaborate on the results of the Anderson and Steenpass studies and how the present study complements these. See above.

lines 15/16: why do you think that LST is only relevant to determined HRUs under radiation-limited conditions? Deleted.

line 21: what do you mean by "transformed images"? Changed to recoded. It is too early to explain the recoding here but necessary to note the procedure.

line 25: no comma after "surface characteristics" Deleted.

page 7023:

line 8: replace "Research" with "research" Changed.

line 19: explain "VNIR" and "SWIR", or remove Explained in the brackets.

page 7024:

lines 1/2: please ensure that order of Figures is consistent with appearance in the text (also when referring to Figures 5 and 6, and 8 and 9 later on), or remove reference to Figure We try to avoid duplicated figures and want to strengthen the rationale in the adequate section. Unchanged.

line 5: explain "L1A", or remove We repeat the initial declaration.

line 10: explain "digital numbers" We added "unprocessed". "Digital number" is the common nomenclature in this context.

line 11: explain "sensor decay" Clarified.

line 16: so you are assuming TOA=LST? under which circumstances can this be valid? please discuss It is already discussed that the used bandwidth is "least altered" due to the atmosphere (Sect 2.2) and that "homogeneous atmospheric conditions" are assumed (Sect. 2.3) hence, patternwise, TOA is closest to LST as possible.

line 22: I do not understand this ratio, please explain or remove Restated.

page 7025:

Please explain in more detail why you are investigating persistence here. And please clarify that you refer to spatial persistence (?). Further, you should elaborate on the choice of your methods; e.g. why not just correlating the images to infer spatial pattern similarity? We added an adequate rationale to Sect. 3.1, as noted above. The overall pattern persistency is stated to be a persistency along the time series, a temporal persistency. The pattern dynamics persistency includes locally spatial information, stated as well. We did not mention "simpler" methods as patterns disregarded. This now is clarified in Sect. 3.1.

line 16: explain "co-referencing", or remove This is used in textbooks as well as specific nomenclature from the cited Hirschmüller et al.. Changed to a citation.

page 7027:

Please clarify that Fig 5 is using artificial data. Changed.

page 7028:

lines 10/12: I guess you mean row here instead of column Changed.

page 7030:

What is the added value of the behavioral measure analysis as compared to the PCA results? There is no accountable "added value", though the method is in line with the rationale on functionality. See rationale above.

line 21: I guess you mean Fig 11 Changed.

Figures 2,3,5,8,9,11 are hard to read, please enlarge captions and labels Changed. (Images will be uploaded as a supplement)

b. Referee 2

I agree with the first reviewer comments, for example on the need for a stronger and more clearly explained rationale for why these methods in particular were selected. In the main the author responses have addressed these, so I will not repeat them here, but I do urge the authors to be very clear in explaining why they have done what they have done.

See above.

Thus overall I find the paper well written and very interesting. I have only a few minor comments:

I think the paper would be stronger with a little bit more context about why HRUs are so important in hydrology, and how they work and what they mean for improving prediction.

What is the background for spatial pattern analysis in addition? A further paragraph in the literature review would much improve this context and thus also help to highlight the importance of this work for hydrological prediction. I think the importance could also be further highlighted in the abstract and conclusions. Don't undersell your work!

We extended the section on HRUs and hence the analysis of patterns, citing appropriate literature. We also added information on the use of persistency measures (see above),

Linked to this I think the authors could give more explicit ideas on how their techniques can be practically turned into improvements in the "conceptualization and parameterization of land surface models and the planning of observational networks within a catchment" Can you suggest some suggested future experiments to make this a reality?

We note the MPR approach of Samaniego et al. considering conceptualization and parameterization and extended the use of delineated Units in the process of planning a monitoring/field campaign.

Please provide more details on the hydrological, ecological and climatological regime of the test site, then link this further to the section where you discuss the transferability of the technique.

We improved the information on the test site (Sect. 2.1). The methods are supposed to be applicable to remote (ungauged) catchments, as noted, hence special explanation on transferability is not further outlined.

2. *Marked-up manuscript version showing the changes made*

See following pages:

1 Identification of catchment functional units by time series 2 of thermal remote sensing images

3
4 B. Müller^{1,2}, M. Bernhardt² and K. Schulz¹

5 [1]{Institute of Water Management, Hydrology and Hydraulic Engineering, University of
6 Natural Resources and Life Sciences, Vienna, Austria}

7 [2]{Department of Geography, Ludwig-Maximilians—~~University-Universität~~, Munich,
8 Germany}

9 Correspondence to: B. Müller (b.mueller@iggf.geo.uni-muenchen.de)

10 11 Abstract

12 The identification of catchment functional behavior with regard to water and energy balance
13 is an important step during the parameterization of land surface models.

14 An approach based on time series of thermal infrared (TIR) data from remote sensing is
15 developed and investigated to identify land surface functioning as is represented in the
16 temporal dynamics of land surface temperature (LST).

17 For the meso-scale Attert catchment in midwestern Luxembourg, a time series of 28 TIR
18 images from ASTER (Advanced Spaceborne Thermal Emission and Reflection Radiometer)
19 was extracted and analyzed—applying a novel process chain:

20 ~~The~~First, the application of mathematical-statistical pattern analysis techniques demonstrated
21 a strong degree of pattern persistency in the data. Dominant LST patterns over a period of 12
22 years were then extracted by a principal component analysis. Component values of the two
23 most dominant components could be related for each land surface pixel to vegetation/land use
24 data, and geology, respectively. ~~A classification~~ The application of ~~the landscape by~~
25 ~~introducing~~ “a data condensation technique (“binary word”, representing words)” extracting
26 distinct differences in the LST dynamics, allowed the separation into functional landscape
27 units that show similar functioning/behavior under radiation driven conditions.

28 It is further outlined that both information, component values from PCA as well as the
29 functional units from “binary words” classification, will highly improve the conceptualization

1 and parameterization of land surface models and the planning of observational networks
2 within a catchment.

3 **1 Introduction**

4 Resolving the spatial variability of hydrological processes at the land surface within spatially
5 explicit physical-based models is still nowadays a very time-consuming and expensive task
6 that is not applicable for operational purposes. Therefore, a large variety of hydrological
7 models is based on the delineation of spatially distributed hydrological functional units that
8 are assumed to behave or function in a similar way for some given initial or boundary
9 condition (Flügel, 1995a). ~~These~~They are often ~~called~~referred to as “hydrological response
10 units (HRUs)” ~~typically~~and represent ~~areas~~classes of ~~homogeneous topography, pedology,~~
11 ~~vegetation and landscape/catchment entities that share common~~ climate conditions that are
12 delineated by intersecting available GIS (Geographic Information System) or remote sensing
13 information/maps, land use and underlying pedo-topo-geological characteristics.

14 In this way the number of computational units is significantly reduced, thus facilitating an
15 efficient parameterization and calculation process. Examples of hydrological model systems
16 following the HRU concept are the “Soil Water Assessment Tool (SWAT)” (Arnold et al.
17 1998; Srinivasan et al., 1998), the Cold Region Hydrological Modell (CRHM) (Pomeroy et
18 al., 2007) or the “Precipitation Runoff Modeling System/ Modular Modeling System
19 (PRMS/MMS)” (Flügel, 1995b), amongst many others. ~~In this way, the definition of HRU’s~~
20 ~~is based on information that is~~While the HRU concept has been criticized in the past for e.g.
21 often neglecting the lateral exchange processes that are driven by inter-unit gradients
22 (Neumann et al., 2010), Zehe et al., (2014) have recently extended the original HRU concept
23 by “postulating a hierarchy of functional units, lead topologies and elementary functional
24 units compiling the main catchment functions in a given hydrological setting by spatially
25 organized interactions at and across different scales”.

26 In any of these concepts the delineation of HRUs or functional units is mainly based on
27 information that is directly related to land and subsurface characteristics that are well known
28 to have some control on a wide range of hydrological processes (such as geology on soil type,
29 soil texture and therefore hydraulic conductivity; or slope on the hydraulic gradient), but that
30 do not represent directly internal states or (water) fluxes.

31 In order to characterize ~~the~~this spatial (hydrological) functioning of the landscape at larger
32 scales, it would be beneficial to have relevant information at hand that will be available

1 routinely (and also at locations that are ungauged) via remote sensing. Typical
2 data/parameters are digital elevation models (DEM) from Radar Missions (Farr et al., 2007;
3 NASA, 2009), land use/land cover data (EEA, 2014; EPA, 2007), as well as soil parameters
4 (Lagacherie et al., 2012; Mulder et al., 2011; Summers et al., 2011; Ladoni et al., 2010; Kheir
5 et al., 2010; Serbin et al., 2009a, 2009b; Eldeiry et al., 2010) from sensors within the visible
6 and near infrared spectrum. ~~Except for phenology or leaf area index data, both representing an~~
7 ~~aggregate response of vegetation to climate, soil moisture and nutrient availability, most of~~
8 ~~these parameters are again indirect indicators of hydrological processes.~~

9 Another important spatial information that can be obtained from remote sensing is land
10 surface temperature (LST). It results from a complex balance and interaction of incoming and
11 outgoing short and long wave radiation as well as sensible, latent and ground heat fluxes
12 (Moran, 2004). Therefore, LST is highly controlled by geographic location, atmospheric
13 ~~states, and state~~, soil (moisture) and vegetation conditions. The monitoring of LST at the
14 catchment scale via thermal infrared (TIR) remote sensing from e.g. LANDSAT (spatial
15 resolution: 4/5 – 120 m, 7 – 60 m, 8 – 100 m), ASTER (90 m) or MODIS (1 km) has been
16 used in the past primarily to derive sensible and latent heat fluxes (Bolle et al., 1993; Farah
17 and Bastiaanssen, 2001). Given the control of latent heat fluxes by the available water content
18 (and therefore by hydraulic properties of the soil, the location within the catchment ~~(~~, Beven
19 and Kirkby, 1979~~)~~, and the phenological and physiological states of the plants ~~(~~, Taiz and
20 Zeiger, 2010~~)~~), TIR data have also been applied to ~~inversely extract estimate~~
21 properties, bulk density or volumetric water content using complex soil-vegetation-
22 atmosphere transfer (SVAT) schemes (e.g. ~~Anderson et al., 2011~~; Steenpass et al., 2010).

23 In this way, LST can be seen as a complex ecosystem state variable that aggregates a variety
24 of (micro-)meteorological and hydrological processes as well as land surface characteristics at
25 each individual pixel in a catchment. The spatio-temporal dynamics of LST is therefore
26 important information in order to distinguish spatially different functional behavior of the
27 landscape, ~~particularly under radiation driven conditions.~~

28
29 In the following, the dynamic patterns of LST are investigated for the ~~288km~~288 km² Attent-
30 catchment in Luxembourg using 28 ASTER (Advanced Spaceborne Thermal Emission and
31 Reflection Radiometer) TIR remote sensing images over a time period of 12 years. The
32 persistency of the LST pattern time series is analyzed in two different novel ways deriving

1 summary statistics of the correlation of shifted windows across the original or
2 ~~transformed~~recoded images and/or time steps (overall pattern persistency, pattern dynamics
3 persistency). The following principal component analysis (PCA) of the LST pattern time
4 series allows the identification of dominant independent patterns within the time series,
5 ranked by the ability/degree to explain the temporal variation in the LST time series. Relating
6 the dominant principal components to available land surface characteristics, will allow to
7 extract the most important controls of LST variation in the catchment under study ~~and~~;
8 Finally a novel scheme is suggested to group pixels/sites related to into a manageable number
9 of functional units based on their ~~eco-hydrological functioning~~—“behavior” that is expressed
10 in a binarized form of LST dynamics for a representative subset of images.

11 The rest of the paper is organized as follows: Section 2 will introduce the test site, the data
12 used and the pre-processing steps necessary. Section 3 will describe the methods applied as
13 well as results in a stepwise approach. Finally, Section 4 summarizes and discusses main
14 findings and gives an outlook to future research.

15

16 **2 Data and Preprocessing**

17 **2.1 Test site**

18 The study area is the Attert catchment located in midwestern Luxembourg and partially in
19 Belgium (see Fig. 1). It is the main test site of the German DFG ~~Research~~research project
20 CAOS (“catchments as ~~organized~~organised systems”, (CAOS, 2014)) with a total catchment
21 area of 288 km² at the gauge in Bissen. The undulating landscape with a mean slope of 8.4%
22 spans between 222 m and 535 m a.s.l. The northern slopes are geologically defined by schists
23 from the Ardennes massif, while the mainly southern slopes arise on sandstones from the
24 Paris basin Mesozoic deposits (compare Fig. 9). Soils vary between sand and silty clay loam.
25 The land cover of the catchment is predominantly cultivated with 4.8% settlements and rather
26 impermeable, 65.4% agricultural used land predominantly on the knolls, and 29.7% forests
27 predominantly in the v-shaped valleys (compare Fig. 9). Climate is characterized by mean
28 monthly temperatures between 18 °C in July and 0 °C in January (1971–2000). The mean
29 annual precipitation is 850 mm (1971–2000); ~~the hydrological regime is defined as and the~~
30 mean annual actual evapotranspiration is 570 mm (1971–2000) resulting in a pluvial oceanic

1 with low flows within July to September due to high summer evapotranspiration, and high
2 flows mainly from December to February.

3 **2.2 Spatial data**

4 The multispectral imaging system ASTER (advanced spaceborne thermal emission and
5 reflection radiometer) on board the TERRA satellite, launched in December 1999, orbits on a
6 near circular, sun-synchronous path with a repeat cycle of 4-16 days. The ASTER instrument
7 consists of three sensors (VNIR, visible-near infrared: 0.52-0.86 μm ; SWIR, shortwave
8 infrared: 1.6-2.43 μm ; TIR, thermal infrared: 8.125-11.65 μm) with 4, 6 and 5 bands,
9 respectively (Fujisada, 1995). For this study, only the Level 1A (raw) TIR data band 13,
10 within 10.25-10.95 μm , with a spatial resolution of 90 m are used. This band is chosen due to
11 the lowest absorption of the atmosphere and, therefore, least altered thermal signals (compare
12 Elder and Strong (1953)). The local overpass time is around 11:40 am LTCET. Between
13 January 2001 and June 2012, a total of 28 snow free images (see Fig. 2, after preprocessing)
14 with a maximum cloud cover of 15% were extracted. In addition, Corine land cover (EEA,
15 1995) updated from 2006 (Fig. 9, upper right), and a geological map based on dominant rock
16 formations (SGL, 2003) (Fig. 9, lower right) are used for further analysis.

17 **2.3 Preprocessing**

18 The ~~delivered L1A~~used Level 1A (raw) TIR data product lacks a proper geo-referencing. This
19 was applied manually with 60 to 70 ground control points (depending on the cloud cover)
20 achieving a mean accuracy of 40 m within the Attert catchment. In this transformation step,
21 the spatial resolution of the images was adjusted from 90 m to 15 m by assigning the nearest
22 neighbor values. The geo-positioned images were then converted from unprocessed digital
23 numbers to top-of-atmosphere temperatures T_{TOA} with standard parameters as given by
24 CESSLU (2009). Sensor decay was not taken into account as decay errors due to spatially
25 homogeneous and heterogeneous degradation of the sensor (sensitivity) are a magnitude
26 smaller than measurement accuracy, according to Hook et al. (2007). Merely homogenous
27 atmospheric conditions throughout the catchment were assumed for each single time step and
28 as our focus is on statistical pattern analysis rather than on absolute LST values, atmospheric
29 correction was omitted here and T_{TOA} is used in the following. Additionally, calculating cloud
30 masks was omitted as heavy fragmentation of the full time series would occur, if masks were
31 applied for even small clouds in every affected image and cumulatively applied for the full

1 series. In further statistical analysis the distortion of results due to clouds is negligibly small
2 as occurring clouds are neither repeating in certain areas nor of large spatial extent per image.
3 The time series of LST for individual pixels in the dataset hence include one outlier due to
4 clouds at most. This ~~means a maximum cloud noise to emittance ratio of 1:27 and~~ does not
5 heavily influence further calculations on the full pattern. For simplification reasons the
6 calculated data is further referred to as LST time series.

8 **3 Methods and Analysis**

9 The general objective was to explore the relevance of the spatio-temporal dynamics of land
10 surface temperature as a determinant of the functional behavior of the water and energy
11 balance of a landscape unit in a given watershed. In the first part of the analysis, the
12 persistency of the LST patterns, both, in a temporal, as well in a spatio-temporal context, was
13 explored- to analyze the existence of spatially and temporally consistent patterns. The second
14 part will analyze the most dominant structures/patterns in the landscape that can be extracted
15 from LST time series using PCA and will also investigate the relationship between dominant
16 structures from LST-PCA and other landscape characteristics. In the third part, landscape
17 functional units will then be classified based on the PCA results.

18 **3.1 Overall pattern persistency**

19 The first aim was to demonstrate that LST patterns, although changing throughout time,
20 persist to a certain degree and, hence, provide information on the local organization of land
21 surface energy and water balance within the full catchment. The absence of persistency would
22 imply competing patterns within the time series and hence sever changes within the
23 controlling features or even oscillating states within the time series. A further investigation of
24 the timing of the pattern changes and appropriate splitting of the time series would be
25 imminent to a comprehensive pattern analysis. In such a case, the following steps need to be
26 executed for the separated datasets. In order to analyze the overall pattern persistency within
27 the time series while retaining spatial patterns a procedure similar to the one used for “co-
28 referencing” different ASTER TIR bands is used (Hirschmüller et al., 2002). The correlation
29 of shifted windows within two images indicates, whether there is a clear shift within the
30 overall pattern in any spatial direction or if “blurring” occurs and, hence, persistency is
31 absent. Therefore, a square window w of defined size w (e.g. 3×3 pixel (px)) around a pixel P_c

1 of the image I_1 (time step 1) is selected and the correlation coefficient is calculated for the
2 same window (e.g. from $3^2=9$ values) in the image I_2 at time step 2 (Fig. 3a). The window
3 within the second image now is shifted around P_c within defined maximum ranges r_1, r_2 (e.g.
4 $r_1=[-3,+3]$ in N-S direction, $r_2=[-3,+3]$ in E-W direction); Fig. 3b) and correlation coefficients
5 are assigned for any shifted position (dx,dy) of P_c and produce square fields of correlation
6 coefficients (e.g. 7×7 px; Fig. 3c).

7
8 The persistency of the patterns in the LST data within two time steps is then assessed by
9 calculating average correlation coefficient fields for a sample of well distributed central
10 pixels, depending on the ratio of window and shift size to image size (to reduce the effort of
11 calculating a shift for the whole image). The overall persistency of the patterns is the average
12 of the correlation coefficients for all combinations of patterns within the time series ($28\cdot(28-$
13 $1)=756$). In case the maximum correlation coefficient is within a shift of (0,0) and the
14 decrease of the correlation coefficients is large towards bigger shifts (= no “blurring” of a
15 single peak), the persistency of the overall pattern over time is considered as high.

16 For our LST time series, the observed overall patterns are stationary persistent in general. By
17 calculating the mean correlation coefficient within the full time series dataset and a range of
18 shifts of $[-50,+50]$ in both directions (Fig. 4), it is shown that the peak correlation value is
19 within a shift of (4,1) px and, hence, within the range of the resolution of one original ASTER
20 pixel (4×15 m=60 m). Also, the overall positioning of temperature values within the patterns
21 is correlated over times and as a first result it can be derived that temporal trends within the
22 thermal images of the Attert catchment can be considered as “spatially stationary persistent”.

23 **3.2 Pattern dynamics persistency**

24 | In addition to the overall persistency, the temporal dynamics of local **THR_{LST}** patterns are
25 investigated using a second type of “moving window” approach. To analyze the spatial
26 relationship of each pixel within its local neighborhood, for each pixel P_c within an image a
27 square window w (the environment) of a defined size (e.g. 3×3 px) around this central P_c is
28 compared to the value of P_c . The environment information (ENV) is summarized to statistical
29 information in the form of percentages of values within the square window that are bigger
30 than, smaller than or equal the value of P_c (see Fig. 6a for an example analysis of values that
31 are bigger than P_c).

1 The variations of the ENV information over time was analyzed for the 28 LST images via the
2 spatial assessment of the coefficient of variation ($|\sigma/\mu|$) for each of the three setups (<, =, >;
3 see example in Fig. 5c-d). The three spatially distributed coefficients of variation are finally
4 reduced to an average pattern of coefficients of variation by taking the mean value of the three
5 setups (Fig. 5b, right).

6 Low coefficients of variation over time indicate a very “stable positioning” or rank of that
7 particular pixel within its local environment. An extreme value of zero would mean no change
8 of dynamics over time for the pixel environments; for a value of 1, the standard deviation is as
9 large as the mean value, suggesting that the persistency of the local pattern is rather low and
10 values larger than 1 have to be interpreted as non-persistent. In this way, areas of low
11 coefficients indicate stable, persistent local patterns and distinct varying behavior can be well
12 identified by areas of high coefficients of variation.

13
14 The analysis of the LST time series using a window size of $15 \times 15 \text{ px} = 225 \times 225 \text{ m}^2$ identifies
15 relatively low coefficients of variation (Fig. 6) with 90% of the values between 0.19 and 0.55,
16 50% within the range of 0.27 and 0.42, and only 0.03% of the values larger than 1. This
17 indicates a high local pattern persistency.

18
19 Based on both, global and local persistency analysis, relatively stationary patterns at the
20 catchment scale, accompanied by stationary dynamics at the scale of hill slopes throughout
21 the catchment can be expected. The existence of LST pattern persistence also suggests some
22 structured control on LST by some land surface characteristics. In the following section
23 possible controls will be extracted and analyzed.

24 **3.3 Principle component analysis**

25 ~~Assessing independent structures is possible by applying~~Applying principle component
26 analysis (PCA; for a full mathematical description, see Richards and Jia (2006; chapter
27 6.1)), ~~or empirical orthogonal functions (EOFs, e.g. Denbo & Allen, 1984; Hamlington et~~
28 ~~al., 2011; Lorenz, 1956) allows the assessment of independent structures within complex data~~
29 ~~sets. Because both approaches share a similar methodology, here,~~ PCA is used to determine
30 which spatial factors are controlling patterns of LST within the time series. PCA uses

1 orthogonal transformation to calculate a composition of linearly uncorrelated values of
2 decreasing dominance from possibly correlated monitored variables. In remote sensing, PCA
3 is often applied to reduce the number of (correlated) variables within classification procedures
4 (see e.g. Crósta et al., 2003; Moore et al., 2008, for the analysis of multi-spectral, single
5 temporal TIR data to assess different geological structures).

6 Here, the aim is to transform the observed 28 LST patterns into patterns of virtual and
7 independent principal components. These components represent the most dominant
8 controlling factors for the temporal dynamics of LST pattern in decreasing order. An
9 illustrative example for a PCA application in this context is given in Fig. [77 for artificial data](#).

10

11 The PCA application for the ASTER TIR time series produced 28 independent components as
12 summarized in Table 1. By construction, components with higher (lower) degree show less
13 (more) information and more (less) noise. 61.9% of the variation is cumulatively expressed
14 via the first 5 components (third [column](#)), while still more than 3% of the variance are
15 expressed by particular components (second [column](#)). In the following, a focus is given to
16 the first 5 components (Fig. 9).

17 Figure 8 illustrates a distinct degree of structured heterogeneity for these 5 components. In
18 principle the patterns of the PCs would allow to classify the catchment/landscape into
19 different functional units that, when using LST images, would strongly reflect the functioning
20 of the landscape related to the water and energy balance under radiation driven conditions.
21 The number of PCs to be considered in such a classification would depend on the overall
22 number of units that should be differentiated (which will strongly depend on computational
23 resources available to explicitly represent within catchment variability), but also on the
24 (cumulative) percentage of explained variance of the PCs, as well as on the distribution/range
25 of the component values of each individual PC.

26 However, while this is an important topic related to land surface hydrological modeling, the
27 focus here will be on the relationship of the extracted PCs with other land surface
28 characteristics. Given the controls of LST as discussed in the introduction, it is expected to
29 find some relationship of the first dominant PCs with vegetation, soil/geology, elevation,
30 slope, aspect or others. A comparison of the PCs with available data suggested a strong
31 relationship between PC1 and vegetation/land use data, as well as PC2 with geological
32 information. These relationships are illustrated in Fig. 9, where maps PC1 and Corine land

1 cover as well as PC2 and a geological map of the Attert catchment are shown next to each
2 other.

3 A more detailed analysis is given by Fig. 10, where the distributions of component values of
4 PC1 for the individual Corine land use data (Fig. 10a) and of PC2 for the individual
5 geological classes (Fig. 10b) are plotted separately. The diagrams underpin a strong
6 relationship between both components and suggested land surface characteristics. Concerning
7 land cover, low component values of PC1 are shown for artificial areas, medium values for
8 agricultural areas (arable, pastures, complex cultivation and agricultural/natural) and high
9 values for forests. In this way, PC1 might be interpreted as related to similar dynamics in leaf
10 area index (LAI) (see Asner et al, 2003), and therefore the potential for water vapor/energy
11 exchange between the land surface and the atmosphere. The high values for “mineral
12 extraction” can be explained, as the single, relatively small area is surrounded by forests and
13 partially replanted with smaller trees/shrubs during the observed time span.

14 When analyzing the component values of PC2 for the different geological classes, schist areas
15 show distinct different distributions compared to the other (mainly) sandstone areas. Schists
16 with a high proportion of fractures are known for a high water drainage potential compared to
17 the remaining sedimentary geology classes (see Chiang, 1971). The availability of water for
18 transpiration and therefore the splitting of available energy into sensible and latent heat
19 fluxes, resulting in different land surface temperatures are thereby strongly affected. In this
20 sense, PC2 can be interpreted as being related to bedrock information or coupled soil texture.

21 Even though land surface temperature is expected to depend on elevation and other terrain
22 properties, no correlation for PC3 to PC5 (and higher) could be found with any other available
23 observable land surface characteristic pattern and in particular to DEM related variables. For
24 the Attert catchment, the elevation differences are moderate and higher altitudes are related to
25 the Schist areas (see Fig. 1). Thus, some part of a possible elevation effect might be “hidden”
26 in PC2 already. However, for other more mountainous areas, possible relationships might be
27 more pronounced and should be considered and analyzed in detail.

28 In addition to the component values, PCA also provides information on the weight of each
29 component within each single time step through calculation of the specific loadings. Table 2
30 illustrates the first 5 components and their loadings for the analyzed data set. While some
31 dependencies of the sign, mean and standard deviation of the loadings with meteorological or
32 hydrological conditions/states in the Attert catchment are expected, here only the differences

1 in the loadings at individual dates are used to identify a limited number of images that are
2 most distinct in their information content but represent the wide range of LST dynamics over
3 the considered time period. Based on the cumulative Euclidean distance of loadings within the
4 LST time series, a number of 5 exemplary images are selected for further analysis (15 Feb
5 2003, 17 May 2004, 24 May 2004, 27 May 2005, and 27 Mar 2012).

6 **3.4 Behavioral measure**

7 In the following, the temporal dynamics of LST data are analyzed in terms of their “functional
8 behavior” and to classify the catchment into areas ~~of similar~~ units some similarity in this
9 behavior- (functional units). Similar to the analysis of pattern dynamics persistency, the vast
10 data variability is transformed into simple information. Using the 5 most different
11 images/time steps (see Sect. 3.3) the data are binarized using an approach suggested by Hauhs
12 and Lange (2008). The pixels of each image within the time step are separated into values
13 larger than the median value of the image (1) or lower (0) (Fig. ~~1311~~, left). The set of 5
14 binarized images can be aggregated into 5-lettered “words” (Hauhs and Lange, 2008) by
15 concatenating these binary values (see three-lettered example in Fig. 11, right).

16
17 ~~Based on the assumptions made with the PCA, the~~ The order of letters within the “words”
18 represents the response of the land surface to differences in the water and energy balance for
19 each pixel ~~and can therefore be used to classify similarly. These different land surface~~
20 responses refer to differently behaving landscape units.

21 The transformation of the 5 LST images into behavioral “words” results in a (still
22 manageable) number of 32 ($=2^5$) classes throughout the catchment, as illustrated in Fig. 12. In
23 some areas, functional behavior changes over short distances indicating different response of
24 the land surface towards radiation driven conditions; other areas behave very similar over
25 larger spatial extend. These larger clusters are characterized by a constant behavior
26 throughout the subset time series with short interruptions only (e.g. class “00010” only has 1
27 short “break” of length 1). Different “binary words” represent different land surface
28 functioning and therefore allow the delineation of “functional units” (with a focus on the
29 radiation driven conditions) in the (Attert) catchment. Based on results from Fig. 9 and 12,
30 larger units can be found within the forests (e.g. “00000”, “10000”, “00001”), main
31 settlements or frequently bare soils (“11111”), and large pastures (“11011” and “00100”). The

1 heterogeneous areas are more related to periodical land cover changes and represent small
2 scale dominations of processes throughout the time series.

3

4 **4 Conclusions**

5 An alternative way of characterizing land surface functionality based on time series of thermal
6 remote sensing images is introduced. First, it is shown that the overall LST patterns of the
7 time series are spatio-temporally persistent. Second, dominant patterns within the time series
8 were extracted via PCA and could be related to physical ecological features such as land use
9 and geology. Based on these analysis, representative images from the time series were
10 selected to express land surface “functionality” in terms of “binary words” and to classify
11 land surface into different “functional units” that again could be related to existent land use
12 patterns in the catchment. In contrast to the “classical” HRU delineation process, where maps
13 of land surface properties (DEM, land use, soil), that often are generalized, estimated,
14 outdated or interpolated from sparse measures, are intersected and hydrological similarity is
15 assumed for these units, the derived principal components and values as well as the
16 classification with regard to “binary words”, both, represent ‘real’ and ‘on-site’ catchment
17 functional behavior with regard to LST and therefore to the water and energy balance at each
18 location.

19

20 While ASTER data were used here, this approach is applicable to any other platform/sensor
21 providing LST information (e.g. Landsat 8 data, 100 m resolution, TIR). Given the maximum
22 spatial resolution of ca. 100 m in TIR remote sensing, any analysis concerning the size of
23 functional similarity in the landscape is limited to that resolution. Aircraft based TIR sensing
24 might overcome this limitation, but is still not routinely available yet. More global hence
25 coarse patterns can be derived from geostationary satellites (e.g. Meteosat) and might improve
26 spatial representations of global standard datasets for climate modeling, e.g. the FAO (Food
27 and Agriculture Organization of the United Nations) world soil map. By investigating the
28 PCA results for different resolutions, it should also be possible to develop new statistical up
29 and down scaling methods for model parameterizations. This approach is also limited by the
30 number and datesseasonality of available (and almost cloud free) LST images. For the Attert
31 catchment a dataset of 28 LST images was available for a period of ca. 12 years. Using the
32 full ~~data-set~~dataset, any significant land surface changes related to LST are implicitly

1 | contained and expressed in the derived principal components and ~~itstheir~~ values as well as in
2 | derived classification of functional units using “binary words”. An analysis of historic
3 | Landsat images has shown that the land use changes in the Attert catchment have been
4 | minimal over the last 35 years, so that crop rotation by farmers is the most dominant change
5 | over the seasons here. Given an average of not even 3 available images per year for this mid-
6 | latitude region (see Fig. 2), any application of this approach will have to balance between
7 | sufficient temporal coverage in order to capture the relevant LST dynamics of the landscape,
8 | and not covering too many externally driven changes into the procedure.

9 | In order to analyze the number of images required, the PCA and “binary word” classification
10 | was repeated with only down to 6 subsequent images (given the minimum set of 5
11 | images/PCs considered in Sects. 3.3 to 3.4). For all the subsets, results in terms of PCA,
12 | component values and classification were similar when compared to the full LST time series,
13 | indicating, that already a much smaller time period and smaller number of images will be
14 | sufficient to capture landscape functioning with regard to LST. This might change with more
15 | complex catchments/sites. The application of digital numbers instead of extracted LST also
16 | showed almost identical results, so that a proper conversion to LST is in our opinion not
17 | fundamentally needed.

18 | What are the additional benefits of the LST analysis presented here? The analysis of “binary
19 | words” as presented in Sect. 3.4 provides a classification of the catchment into areas that
20 | behave similarly (with regard to the complex interactions of the water/energy balance as
21 | expressed in LST) in terms of response to radiation driven conditions. These units can either
22 | be used in an already established HRU framework or provide some guidance on the size of
23 | spatial discretization of the landscape in land surface modeling exercises, and might support
24 | effective observation-/monitoring strategies under limited resources by providing distributed
25 | information of distinct behavior- and hence be used as decision support on the spatial
26 | distributions of field experiments. The strongest impact of the approach presented is expected
27 | when the derived component values from the PCA analysis will be incorporated into model
28 | parameter regionalization schemes (e.g. the multi-scale parameter regionalization (MPR)
29 | scheme presented by Samaniego et al-~~(., 2010))~~). Rather than providing nominal scaled data,
30 | the component values are continuous, pixel based information representing the land surface
31 | functioning with regard to LST. Formulating the parameterization of land surface models by
32 | e.g. transfer functions (see MPR) that are based on individual component values derived from

1 PCA are expected to strongly improve the spatially explicit modeling of catchment water and
2 energy fluxes. However, this hypothesis has still to be tested by comparing these different
3 regionalization approaches within different models and catchments.

4 By extending this analysis to further catchments under different terrain, climate, and
5 vegetation conditions, it is expected that a more general interpretation and understanding of
6 principal components, component values and loadings and their occurrence and interrelation
7 can be derived. The impact of elevation on LST will certainly be more dominant in
8 mountainous areas; soil texture is supposed to show stronger signals in water limited regions;
9 information on variations within multi-level vegetation will appear in strongly natural and
10 forested areas; and the association of PCA loadings with e.g. meteorological measurements or
11 indices (e.g. cumulative rainfall of the last 7 days) might allow further processes/states (such
12 as interception storage) to be derived.

13

14 **Acknowledgements**

15 We thank the German Research Foundation (DFG) for funding this research through the
16 CAOS (Catchments as Organised Systems) Research Unit (FOR 1598; Grant SCHU1271/5-
17 1).

1 **References** We also want to thank the LPDAAC (Land Processes Distributed Active
2 Archive Center) for providing free ASTER data as well as the editor and anonymous referees
3 for their contributions to improve this article.

4 Anderson, M. C., Kustas, W. P., Norman, J. M., Hain, C. R., Mecikalski, J. R., Schultz, L.,
5 González-Dugo, M. P., Cammalleri, C., d'Urso, G., Pimstein, A., and Gao, F.: Mapping daily
6 evapotranspiration at field to continental scales using geostationary and polar orbiting satellite
7 imagery, Hydrol Earth Syst Sc, 15, 223-239, doi:10.5194/hess-15-223-2011, 2011.

8

1 References

2 Arnold, J. G., Srinivasan, R., Muttiah, R.S., and Williams, J. R.: Large area hydrologic
3 modeling and assessment Part I: Model development, *J Am Water Resour As*, 34, 73-89,
4 doi:10.1111/j.1752-1688.1998.tb05961.x, 1998.

5 Asner, G. P., Scurlock, J. M. O., and Hicke, J. A.: Global synthesis of leaf area index
6 observations: implications for ecological and remote sensing studies, *Global Ecol Biogeogr*,
7 12, 191-205, doi:10.1046/j.1466-822X.2003.00026.x, 2003.

8 Beven, K. J. and Kirkby, M. J.: A physically based variable contributing area model of
9 catchment hydrology, *Hydrological Sciences Bulletin*, 24, 43-69,
10 doi:10.1080/02626667909491834, 1979.

11 Bolle, H.-J., Feddes, R. A., and Kalma, J. D.: (Eds.): Exchange ~~Prøecesses~~processes at the
12 Land-Surfaceland surface for a Rangerange of Spaeespace and Time-Sealestime scales,
13 *Proceedings of Symposium J3.1, Joint Scientific Assembly of IAMAP and IAHS, Yokohama,*
14 *Japan, 11—23 July 1993, 626 pp., 1993.*

15 CAOS: CAOS - Catchments as Organised Systems, <http://www.caos-project.de>, last access:
16 May 22, 2014.

17 CESSLU: How to calculate reflectance and temperature using ASTER data, prepared by
18 Abduwasit Ghulam, Center for Environmental Sciences at Saint Louis University,
19 http://www.gis.slu.edu/RS/ASTER_Reflectance_Temperature_Calculation.php, last access:
20 22 May 2014, 2009.

21 Chiang, S.L.: A runoff potential rating table for soils, *J Hydrol*, 13, 54-62, doi:10.1016/0022-
22 1694(71)90200-9, 1971.

23 Crósta, A.P., De Souza Filho, C.R., Azevedo, F. and Brodie, C.: Targeting key alteration
24 minerals in epithermal deposits in Patagonia, Argentina, using ASTER imagery and principal
25 component analysis, *Int J Remote Sens*, 24, 4233-4240, doi:10.1080/0143116031000152291,
26 2003.

27 Denbo, D. W., and Allen, J. S.: Rotary empirical orthogonal function analysis of currents near
28 the Oregon coast, *J Phys Oceanogr*, 14(1), 35-46, doi:10.1175/1520-
29 0485(1984)014<0035:REOFAO>2.0.CO;2 1984.

1 EEA: CORINE Land Cover Project, published by Commission of the European Communities,
2 <http://www.eea.europa.eu/publications/COR0-landcover>, last access: 22 May 2014, 1995.

3 EEA: Environmental Terminology and Discovery Service (ETDS), published by European
4 Environment Agency,
5 http://glossary.eea.europa.eu/terminology/concept_html?term=corine%20land%20cover, last
6 access: 22 May 2014.

7 Eldeiry, A. and Garcia, L.: Comparison of Ordinary Kriging, Regression Kriging, and
8 Cokriging Techniques to Estimate Soil Salinity Using LANDSAT Images, *J Irrig Drain E-*
9 *ASCE*, 136, 355-364, doi:10.1061/(ASCE)IR.1943-4774.0000208, 2010.

10 Elder, T. and Strong, J.: The infrared transmission of atmospheric windows, *J Franklin I*, 255,
11 189-208, doi:10.1016/0016-0032(53)90002-7, 1953.

12 EPA: Multi-Resolution Land Characteristics Consortium (MRLC), <http://www.epa.gov/mrlc/>,
13 last access: 22 May 2014, 2007.

14 Farah, H. O. and Bastiaanssen, W. G. M.: Impact of spatial variations of land surface
15 parameters on regional evaporation: a case study with remote sensing data, *Hydrol Process*,
16 15, 1585-1607, doi:10.1002/hyp.159, 2001.

17 Farr, T. G., Rosen, P.A., Caro, E., Crippen, R., Dure, R., Hensley, S., Kobrick, M., Paller, M.,
18 Rodriguez, E., Roth, L., Seal, D., Shaffer, S., Shimada, J., Umland, J., Werner, M., Oskin, M.,
19 Burbank, D., and Alsdorf, D.: The Shuttle Radar Topography Mission, *Rev Geophys*, 45,
20 RG2004, doi:10.1029/2005RG000183, 2007.

21 Flügel, W. A.: Delineating Hydrological Response Units (HRUs) by GIS analysis for regional
22 hydrological modelling using PRMS/MMS in the drainage basin of the River Bröl, Germany,
23 *Hydrol Process*, 9, 423-436, doi:10.1002/hyp.3360090313, 1995a.

24 Flügel, W. A.: Hydrological Response Units (HRUs) to preserve basin heterogeneity in
25 hydrological modelling using PRMS/MMS – case study in the Bröl basin, Germany, in:
26 *Modelling and Management of Sustainable Basin-Scale Water Resource Systems*, Boulder,
27 Colorado, USA, 1-14 July 1995, 79-87, 1995b.

28 Fujisada, H.: Design and performance of ASTER instrument, in: *Advanced and Next-*
29 *Generation Satellites*, Proceedings of SPIE, Paris, France, 15 December 1995, 16-25,
30 doi:10.1117/12.228565, 1995.

- 1 [Hamlington, B. D., Leben, R. R., Nerem, R. S., Han, W., and Kim, K. Y.: Reconstructing sea](#)
2 [level using cyclostationary empirical orthogonal functions, J Geophys Res-Oceans \(1978–](#)
3 [2012\), 116\(C12\), doi:10.1029/2011JC007529, 2011.](#)
- 4 Hauhs, M. and Lange, H.: Classification of Runoff in Headwater Catchments: A Physical
5 Problem?, *Geography Compass*, 2, 235-254, doi:10.1111/j.1749-8198.2007.00075.x, 2008.
- 6 Hirschmüller, H., Innocent, P.R., and Garibaldi, J.: Real-Time Correlation-Based Stereo
7 Vision with Reduced Border Errors, *Int J Comput Vision*, 47, 229-246,
8 doi:10.1023/A:1014554110407, 2002.
- 9 Hook, S.J., Vaughan, R.G., Tonooka, H., and Schladow, S.G.: Absolute Radiometric In-Flight
10 Validation of Mid Infrared and Thermal Infrared Data From ASTER and MODIS on the Terra
11 Spacecraft Using the Lake Tahoe, CA/NV, USA, Automated Validation Site, *IEEE T Geosci*
12 *Remote*, 45, 1798-1807, doi: 10.1109/TGRS.2007.894564, 2007.
- 13 Kheir, R. B., Greve, M.H., Bøcher, P.K., Greve, M.B., Larsen, R., and McCloy, K: Predictive
14 mapping of soil organic carbon in wet cultivated lands using classification-tree based models:
15 the case study of Denmark, *J Environ Manage*, 91, 1150-1160,
16 doi:10.1016/j.jenvman.2010.01.001, 2010.
- 17 Ladoni, M., Bahrami, H. A., Alavipanah, S. K., and Noroozi, A. A.: Estimating soil organic
18 carbon from soil reflectance: a review, *Precision Agriculture*, 11, 82-100,
19 doi:10.1007/s11119-009-9123-3, 2010.
- 20 Lagacherie, P., Bailly, J. S., Monestiez, P., and Gomez, C.: Using scattered hyperspectral
21 imagery data to map the soil properties of a region, *Eur J Soil Sci*, 63, 110-119,
22 doi:10.1111/j.1365-2389.2011.01409.x, 2012.
- 23 [Lorenz, E. N.: Empirical orthogonal functions and statistical weather prediction, Scientific](#)
24 [Report No. 1, Statistical Forecasting Project, Department of Meteorology, MIT, 49 pp., 1956.](#)
- 25 Moore, F., Rastmanesh, F., Asadi, H., and Modabberi, S.: Mapping mineralogical alteration
26 using principal-component analysis and matched filter processing in the Takab area,
27 north-west Iran, from ASTER data, *Int J Remote Sens*, 29, 2851-2867,
28 doi:10.1080/01431160701418989, 2008.

1 Moran, M. S.: Thermal infrared measurement as an indicator of plant ecosystem health, in:
2 Thermal Remote Sensing in Land Surface Processes, edited by: Quattrochi, D. A. and Luvall,
3 J., CRC Press, Boca Raton, Florida, USA, 257-282, doi:10.1201/9780203502174-c9, 2004.

4 Mulder, V. L., de Bruin, S., Schaepman, M.E., and Mayr, T. R.: The use of remote sensing in
5 soil and terrain mapping – A review, Geoderma, 162, 1-19,
6 doi:10.1016/j.geoderma.2010.12.018, 2011.

7 NASA: Shuttle Radar Topography Mission, <http://www2.jpl.nasa.gov/srtm>, last access: 22
8 May 2014, 2009.

9 [Neumann, L. N., Western, A. W. and Argent, R. M.: The sensitivity of simulated flow and](#)
10 [water quality response to spatial heterogeneity on a hillslope in the Tarrawarra catchment,](#)
11 [Australia, Hydrol Process, 24, 76–86. doi:10.1002/hyp.7486, 2010.](#)

12 Pomeroy, J. W., Gray, D. M., Brown, T., Hedstrom, N. R., Quinton, W. L., Granger, R. J.,
13 and Carey, S. K.: The cold regions hydrological model: a platform for basing process
14 representation and model structure on physical evidence, Hydrol Process, 21, 2650-2667,
15 doi:10.1002/hyp.6787, 2007.

16 Richards, J.A. and Jia, X.: The Principal Components Transformation, in: Remote sensing
17 digital image analysis: an introduction. 4th ed., Springer, Berlin, Germany, 133-148, 2006.

18 Samaniego, L., Kumar, R., and Attinger, S.: Multiscale parameter regionalization of a grid-
19 based hydrologic model at the mesoscale, Water Resour Res, 46,
20 doi:10.1029/2008WR007327, 2010.

21 Serbin, G., Daughtry, C. S. T., Hunt, E. R., Jr., Reeves III, J. B., and Brown, D. J.: Effects of
22 soil composition and mineralogy on remote sensing of crop residue cover, Remote Sens
23 Environ, 113, 224-238, doi:10.1016/j.rse.2008.09.004, 2009a.

24 Serbin, G., Hunt, E. R., Jr., Daughtry, C. S. T., McCarty, G. W., and Doraiswamy, P. C.: An
25 Improved ASTER Index for Remote Sensing of Crop Residue, Remote Sensing, 1, 971-991,
26 doi:10.3390/rs1040971, 2009b.

27 SGL: Carte Géologique du Luxembourg, Feuille No. 7, Redange, 1:25.000, R. Colpach,
28 Service Géologique du Luxembourg, Luxembourg, 2003.

- 1 Srinivasan, R., Ramanarayanan, T. S., Arnold, J.G., and Bednarz, S. T.: Large area hydrologic
2 modeling and assessment Part II: Model application, *J Am Water Resour As*, 34, 91-101,
3 doi:10.1111/j.1752-1688.1998.tb05962.x, 1998.
- 4 Steenpass, C., Vanderborght, J., Herbst, M., Simunek, J. and Vereecken, H.: Estimating soil
5 hydraulic properties from infrared measurements of soil surface temperatures and TDR data,
6 *Vadose Zone Journal*, 9, 910-924, doi:10.2136/vzj2009.0176, 2010.
- 7 Summers, D., Lewis, M., Ostendorf, B., and Chittleborough, D.: Unmixing of soil types and
8 estimation of soil exposure with simulated hyperspectral imagery, *Int J Remote Sens*, 32,
9 6507-6526, doi:10.1080/01431161.2010.512931, 2011.
- 10 Taiz, L. and Zeiger, E.: *Plant Physiology*, 5th ed., Sinauer Associates, Sunderland,
11 Massachusetts, USA, 782pp., 2010.
- 12 [Zehe, E. and Ehret, U. and Pfister, L. and Blume, T. and Schröder, B. and Westhoff, M. and](#)
13 [Jackisch, C. and Schymanski, S. J. and Weiler, M. and Schulz, K. and Allroggen, N. and](#)
14 [Tronicke, J. and Dietrich, P. and Scherer, U. and Eccard, J. and Wulfmeyer, V., and Kleidon,](#)
15 [A.: HESS Opinions: Functional units: a novel framework to explore the link between spatial](#)
16 [organization and hydrological functioning of intermediate scale catchments, *Hydrol Earth*](#)
17 [*Syst Sc Discussions*, 11\(3\), 3249-3313, 2014.](#)
- 18

1 Table 1: Overview on the 28 calculated principle components (PCs) regarding their accounted
 2 proportion of variance. The components show in each column their specific standard
 3 deviation (σ), proportion of variance (prop. of VAR) and cumulative proportion of variance
 4 (cum. prop.).

	PC1	PC2	PC3	PC4	PC5	PC6	PC7
σ	3.475	1.502	1.018	1.006	0.977	0.874	0.867
prop. of VAR	0.431	0.081	0.037	0.036	0.034	0.027	0.027
cum. prop.	0.431	0.512	0.549	0.585	0.619	0.646	0.673
continued	PC8	PC9	PC10	PC11	PC12	PC13	PC14
σ	0.843	0.834	0.792	0.754	0.746	0.730	0.713
prop. of VAR	0.025	0.025	0.022	0.020	0.020	0.019	0.018
cum. prop.	0.699	0.723	0.746	0.766	0.786	0.805	0.823
continued	PC15	PC16	PC17	PC18	PC19	PC20	PC21
σ	0.712	0.694	0.671	0.669	0.646	0.619	0.598
prop. of VAR	0.018	0.017	0.016	0.016	0.015	0.014	0.013
cum. prop.	0.841	0.858	0.875	0.891	0.905	0.919	0.932
continued	PC22	PC23	PC24	PC25	PC26	PC27	PC28
σ	0.589	0.575	0.555	0.535	0.525	0.483	0.357
prop. of VAR	0.012	0.012	0.011	0.010	0.010	0.008	0.005
cum. prop.	0.944	0.956	0.967	0.977	0.987	0.995	1.000

5

6

1 | Table 2: Loadings of the first 5 components (rows) to reproduce the LST time series
2 | (columns). The weights differ largely between the time steps. The lowest coefficient of
3 | variation for the loadings is calculated for PC1 (0.195), the highest value for PC2 (136.996);
4 | PC3, PC4 and PC5 have coefficients of variation of 80.131, 21.914 and 14.193.

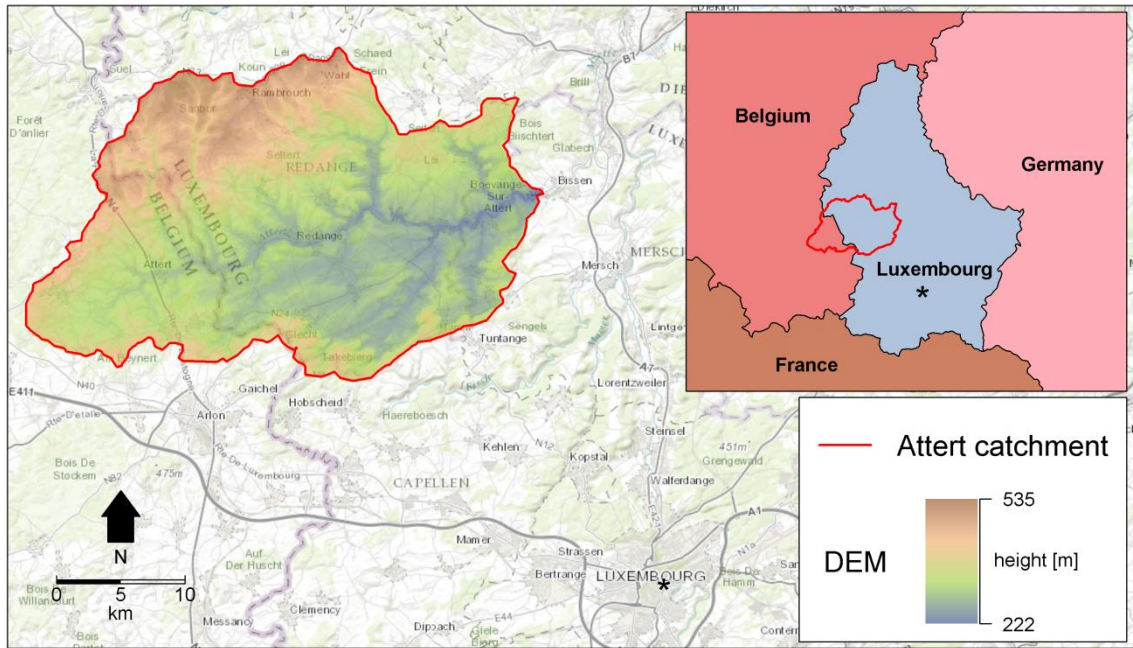
loading of	25 Feb 2001	23 Sep 2001	15 Feb 2003	21 Mar 2003	03 Aug 2003	15 Apr 2004	17 May 2004
PC1	-0.055	-0.056	-0.044	-0.054	-0.052	-0.038	-0.048
PC2	-0.050	-0.038	-0.099	0.012	0.026	0.054	0.023
PC3	0.045	0.006	0.042	0.041	-0.043	0.099	0.057
PC4	-0.066	-0.072	-0.013	-0.054	-0.055	0.009	0.029
PC5	0.059	0.000	0.075	0.016	-0.018	-0.028	-0.098

continued	24 May 2004	27 May 2005	12 Sep 2006	01 May 2007	15 Jul 2008	24 Jul 2008	26 Sep 2008
PC1	-0.056	-0.043	-0.054	-0.049	-0.061	-0.053	-0.055
PC2	0.002	-0.015	0.019	0.045	-0.025	-0.024	0.004
PC3	0.038	0.014	-0.022	-0.024	-0.036	-0.048	-0.022
PC4	0.008	0.041	-0.063	0.006	0.028	0.014	-0.070
PC5	-0.103	-0.085	-0.026	-0.016	-0.011	-0.001	0.004

continued	21 Mar 2009	20 Apr 2009	22 May 2009	23 Jun 2009	02 Jul 2009	27 Jul 2009	16 Apr 2010
PC1	-0.059	-0.038	-0.050	-0.043	-0.042	-0.049	-0.034
PC2	0.026	0.026	-0.041	-0.028	-0.037	-0.033	0.098
PC3	-0.004	0.010	0.007	-0.067	-0.052	-0.022	0.010
PC4	-0.011	0.091	0.061	0.078	0.112	0.008	0.020
PC5	0.042	0.075	0.007	0.049	0.000	-0.006	0.104

continued	23 Apr 2010	23 Sep 2010	19 Apr 2011	30 May 2011	06 Nov 2011	27 Mar 2012	14 May 2012
PC1	-0.037	-0.034	-0.059	-0.059	-0.028	-0.032	-0.048
PC2	0.070	0.057	-0.024	-0.003	-0.117	0.066	0.017
PC3	0.056	-0.128	-0.035	-0.026	0.069	0.038	0.013
PC4	0.027	-0.061	0.031	-0.041	-0.025	-0.010	0.044
PC5	0.022	0.010	-0.014	-0.043	0.038	0.058	-0.013

1

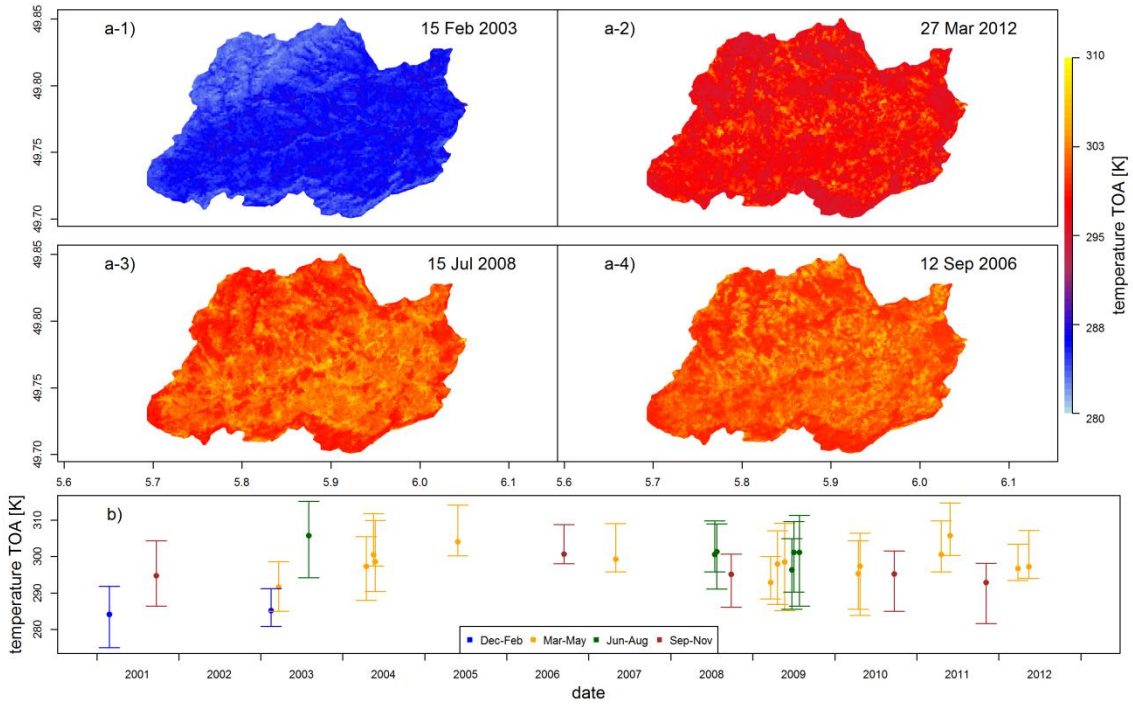


1

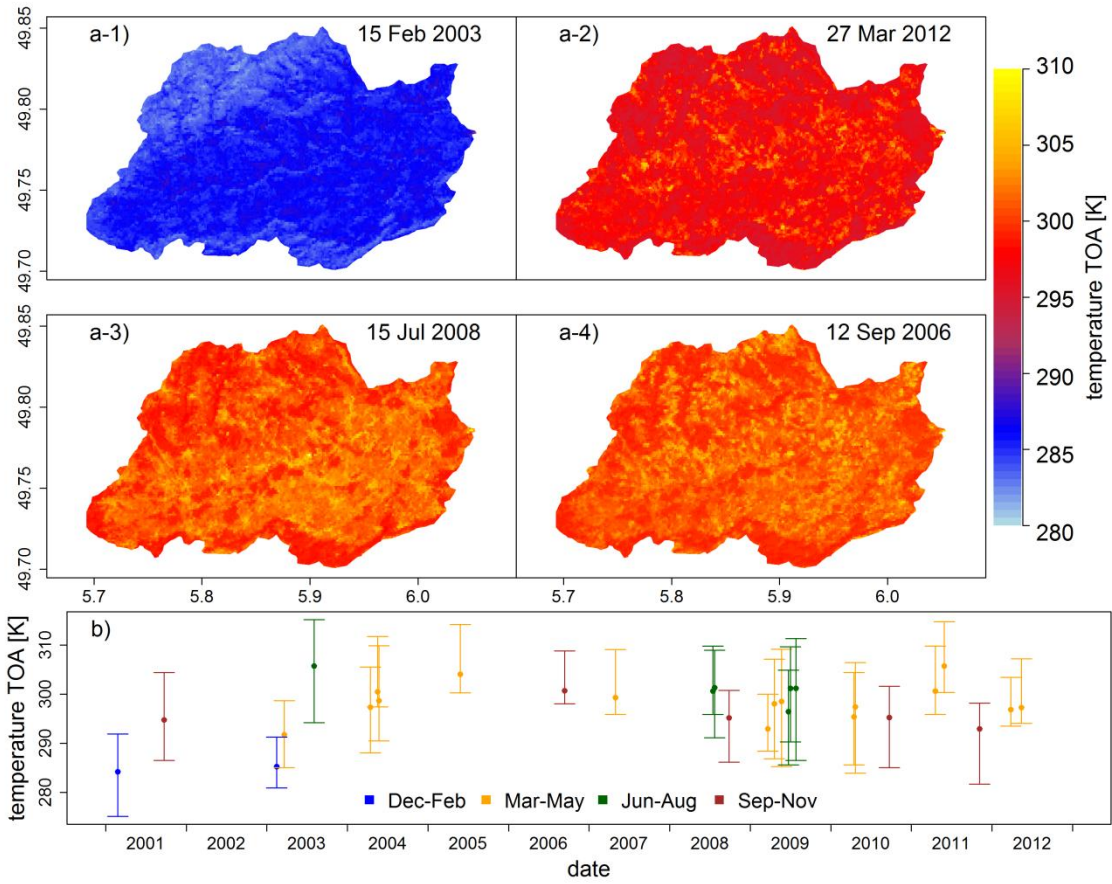
2

3 Figure 1: The location of the Attert catchment and its elevation. Catchment boundaries are
 4 given for the gauge Bissen, Luxembourg.

5



1



2

3

1 Figure 2: a) Examples of single band top-of-atmosphere (TOA) temperature time series
2 covering winter (1), spring (2), summer (3) and autumn (4). b) Basic temporal and statistical
3 information (mean, ranges) of the image time series.
4

$$I_1$$

5	5	4	4	4	4	5	5	6
5	4	4	3	3	4	4	4	5
4	4	3	2	2	2	3	4	4
4	3	3	2	1	0	3	3	4
4	3	2	1	0	1	2	3	4
4	3	2	1	0	1	2	4	4
5	3	3	2	2	2	3	3	5
5	4	4	3	3	4	3	5	5
6	5	4	4	4	4	4	5	6

$$I_2$$

5	4	4	4	4	5	4	5	6
6	4	4	2	3	2	4	4	5
4	3	4	2	2	2	3	4	3
4	4	3	2	1	0	3	3	4
4	3	2	0	0	1	2	2	4
3	2	2	1	0	1	2	4	3
4	3	2	3	1	2	3	2	6
6	4	4	3	3	4	3	5	5
6	5	4	4	4	4	3	5	6

$w P_c$

shift: (0,0)

$$I_1$$

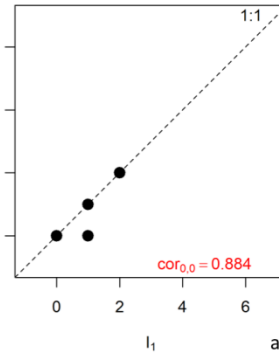
2	1	0	1	0	1	1	0	1
---	---	---	---	---	---	---	---	---

P_c

$$I_2$$

2	1	0	0	0	1	1	0	1
---	---	---	---	---	---	---	---	---

correlation



$$I_1$$

5	5	4	4	4	4	5	5	6
5	4	4	3	3	4	4	4	5
4	4	3	2	2	2	3	4	4
4	3	3	2	1	0	3	3	4
4	3	2	1	0	1	2	3	4
4	3	2	1	0	1	2	4	4
5	3	3	2	2	2	3	3	5
5	4	4	3	3	4	3	5	5
6	5	4	4	4	4	4	5	6

$$I_2$$

5	4	4	4	4	5	4	5	6
6	4	4	2	3	2	4	4	5
4	3	4	2	2	2	3	4	3
4	4	3	2	1	0	3	3	4
4	3	2	0	0	1	2	2	4
3	2	2	1	0	1	2	4	3
4	3	2	3	1	2	3	2	6
6	4	4	3	3	4	3	5	5
6	5	4	4	4	4	3	5	6

$w P_c$

shift: (-3,3)

$$I_1$$

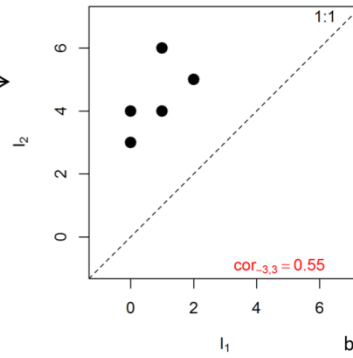
2	1	0	1	0	1	1	0	1
---	---	---	---	---	---	---	---	---

P_c

$$I_2$$

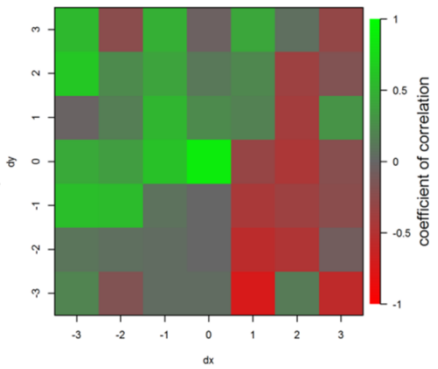
5	4	4	6	4	4	4	3	4
---	---	---	---	---	---	---	---	---

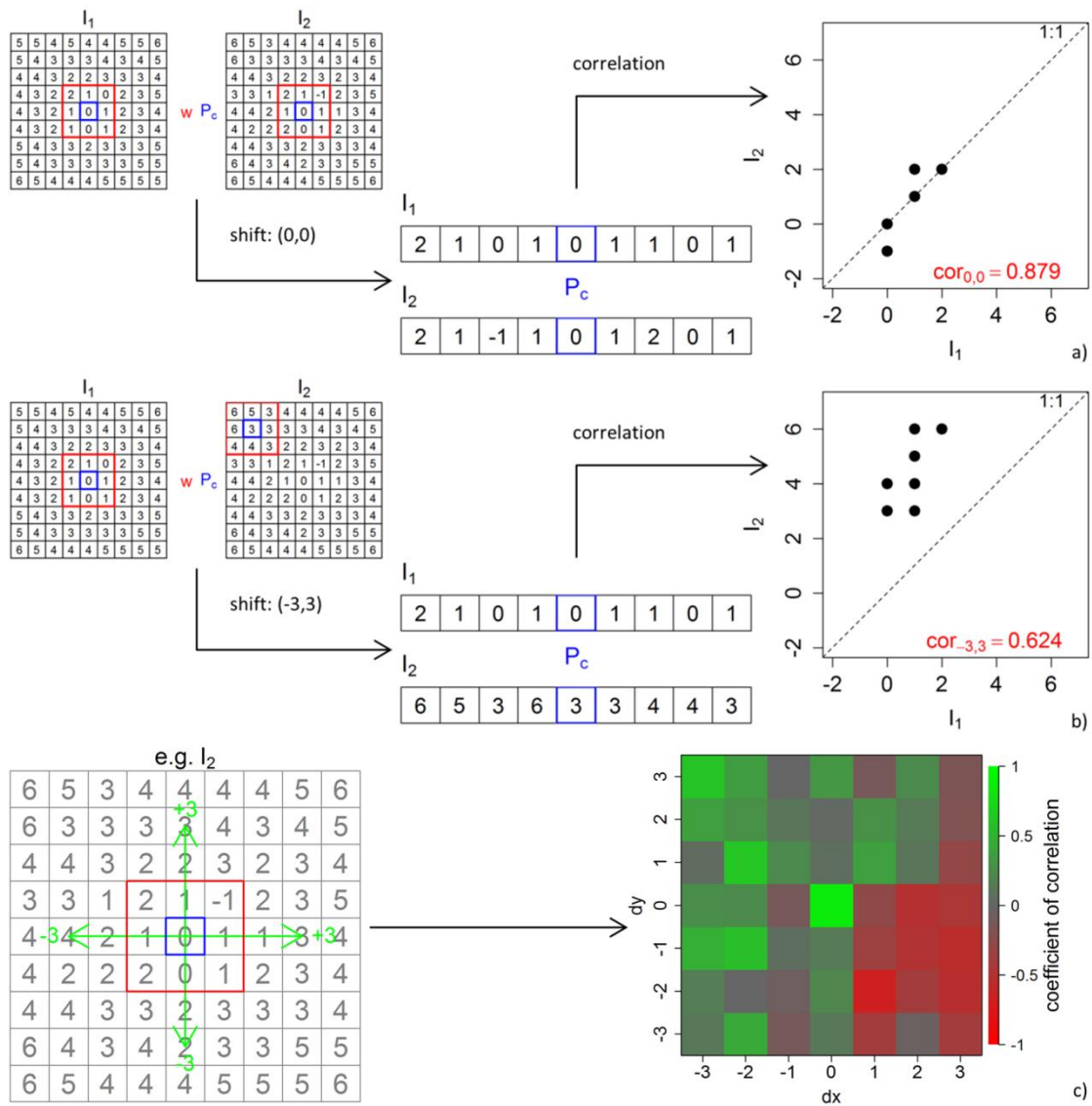
correlation



e.g. I_2

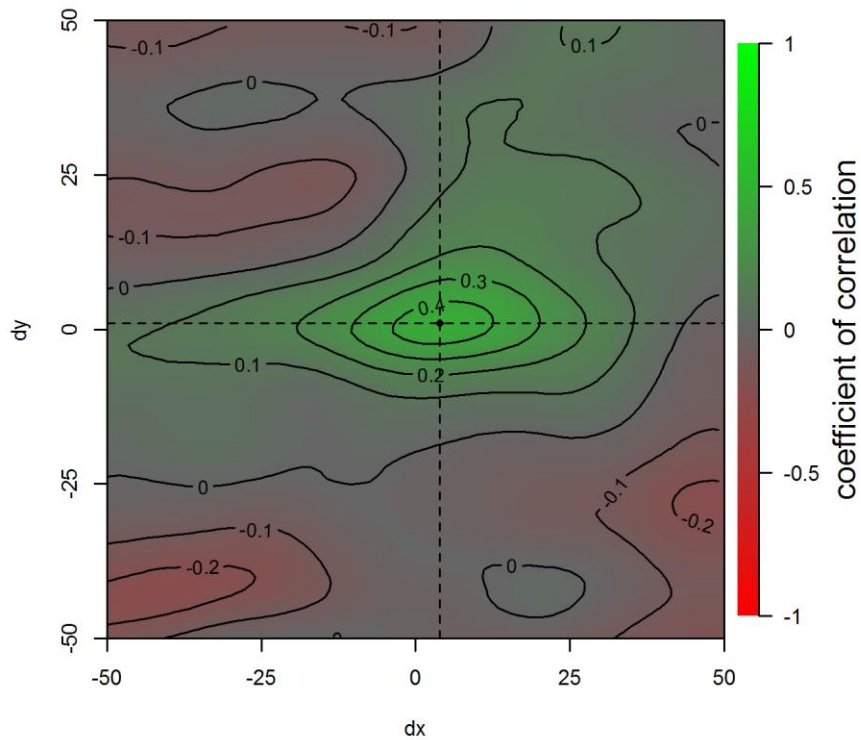
5	4	4	4	4	5	4	5	6
6	4	4	2	3	2	4	4	5
4	3	4	2	2	2	3	4	3
4	4	3	2	0	0	3	3	4
4	-3	2	0	0	1	2	+3	4
3	2	2	1	1	1	2	4	3
4	3	2	3	2	2	3	2	6
6	4	4	3	3	4	3	5	5
6	5	4	4	4	4	3	5	6





1
2
3
4
5
6
7
8

Figure 3: Analysis for the coefficient of correlation for a designed spatial dataset. We added small normal distributed noise to a concentric spatial pattern I_1 to construct I_2 and show the correlation for an extracted window w (red) around the central pixel P_c (blue) in the same position (a), in different positions (b) and for the whole image I_2 within the maximum ranges $[-3,+3]$ (c).

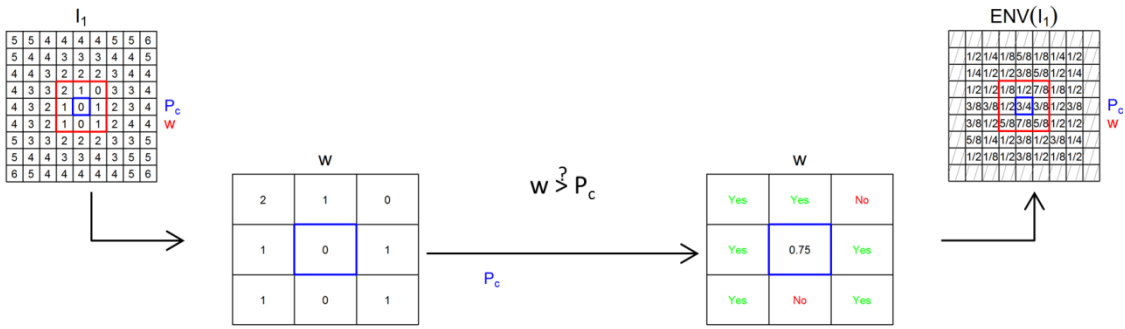


1

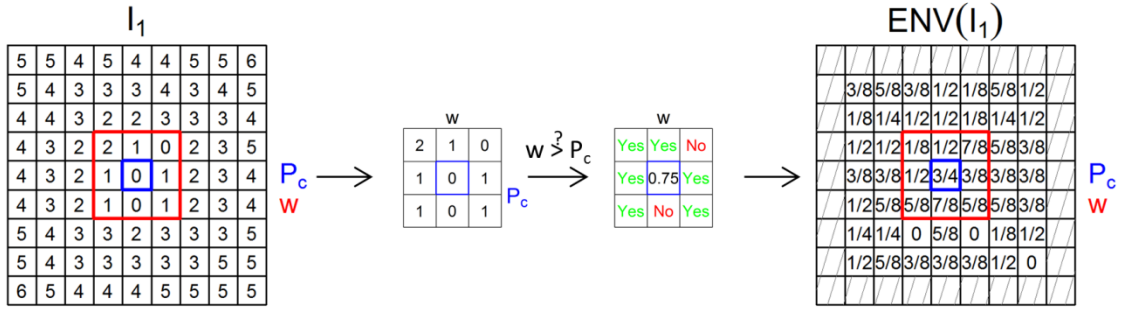
2

3 Figure 4: Coefficient of correlation for the LST time series data. The mean coefficient of
 4 correlation for all 756 combinations shows a centered behavior (single peak area with
 5 maximum correlation of 0.47; green) with a low shift (4,1) within a maximum range of [-
 6 50,+50] in both x- and y-direction. The size of the correlation window is 51×51 px for 5 fixed,
 7 non-overlapping positions ($\begin{matrix} \blacksquare & \blacksquare & \blacksquare \\ \blacksquare & \blacksquare & \blacksquare \\ \blacksquare & \blacksquare & \blacksquare \end{matrix}$) throughout the images.

8



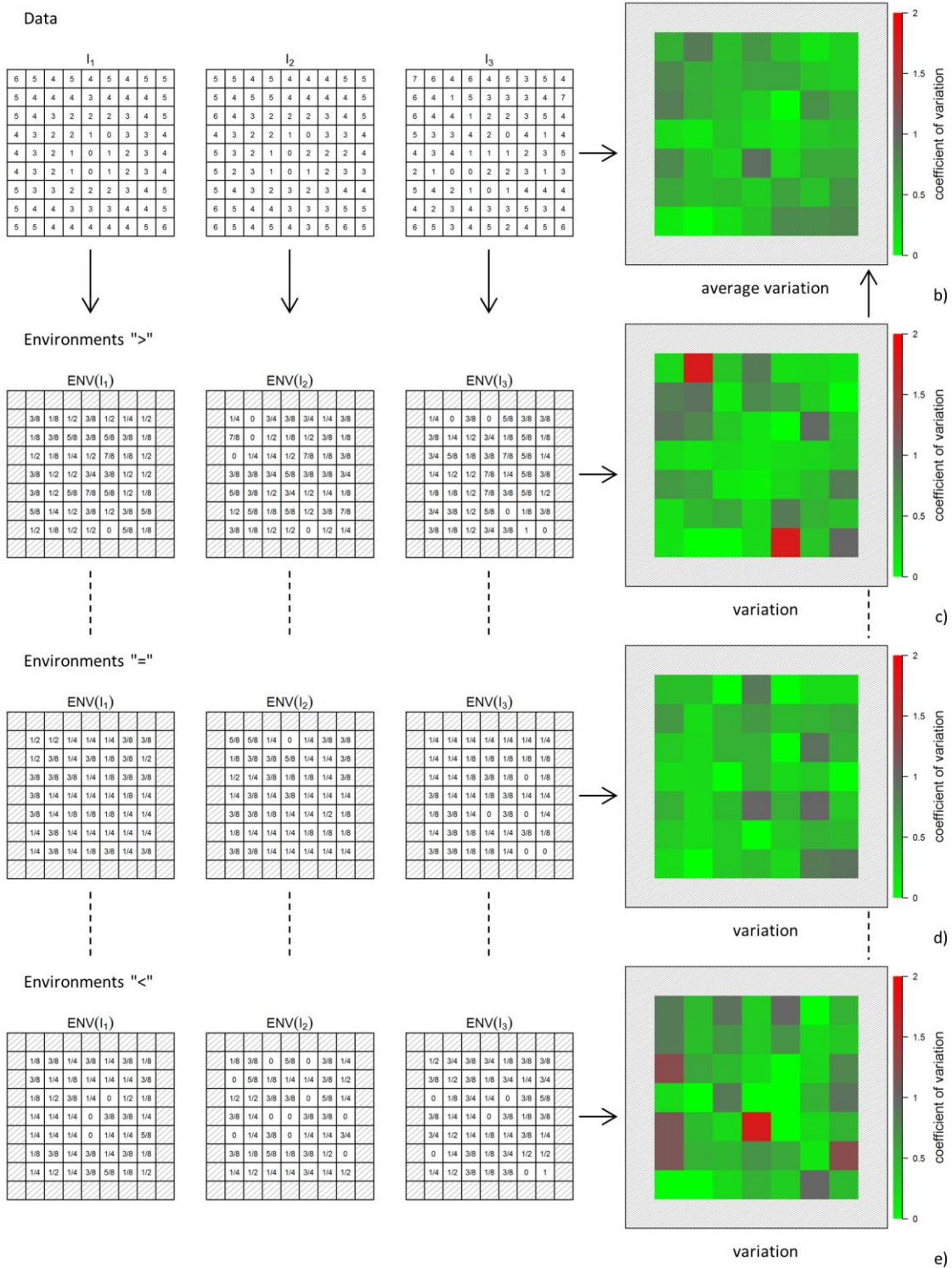
1 a)



2 a)

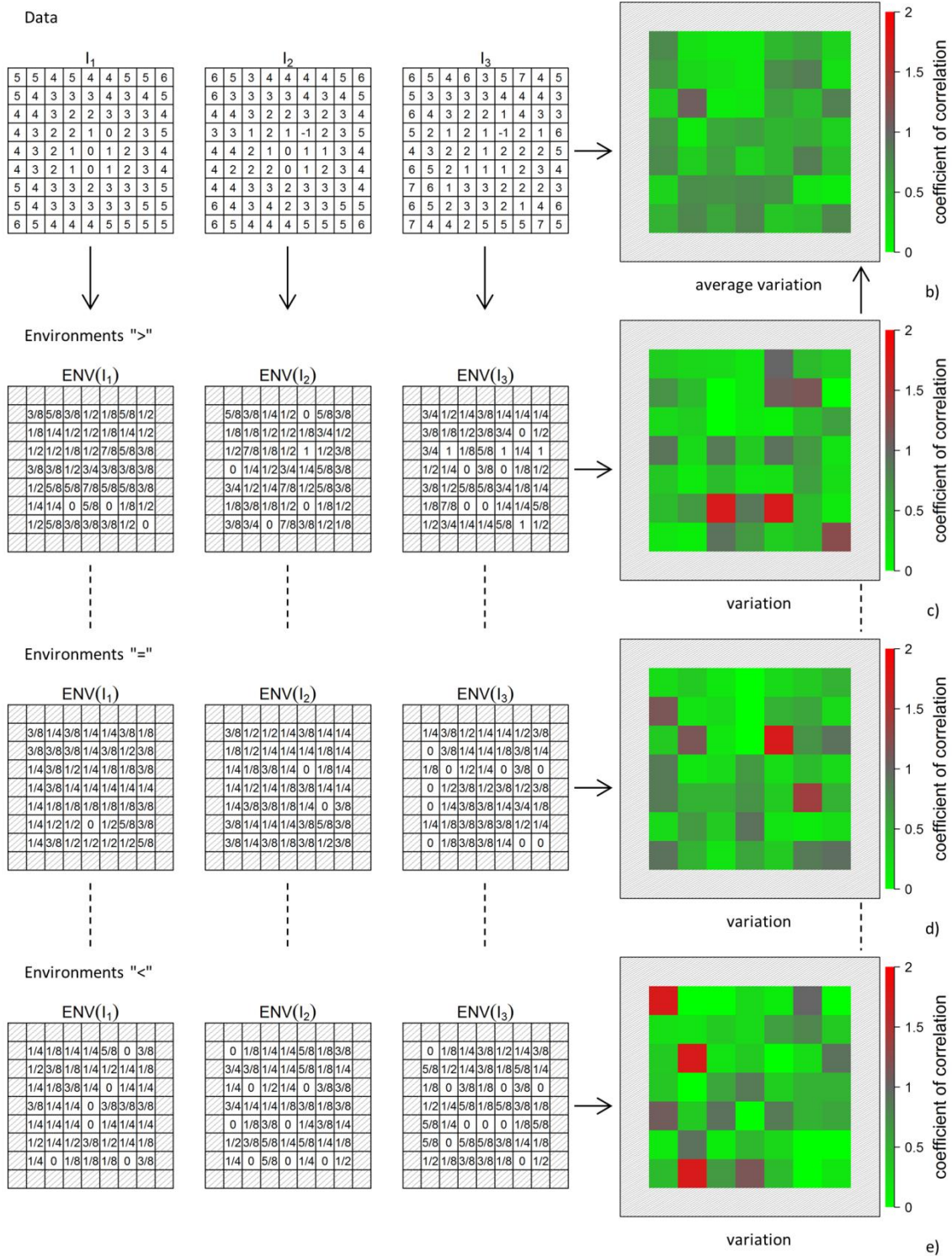
3 Figure 5: Analysis of the coefficient of variation via an “environment assessment” for a
 4 designed dataset. The data are generated in the same way as in the previous analysis (see Fig.
 5 3). Subfigure (a) illustrates the derivation of a single summary value for the central pixel P_c
 6 (blue) from the data of the surrounding environment w (red). The example here investigates
 7 how many values within the environment are larger than the central value.

8



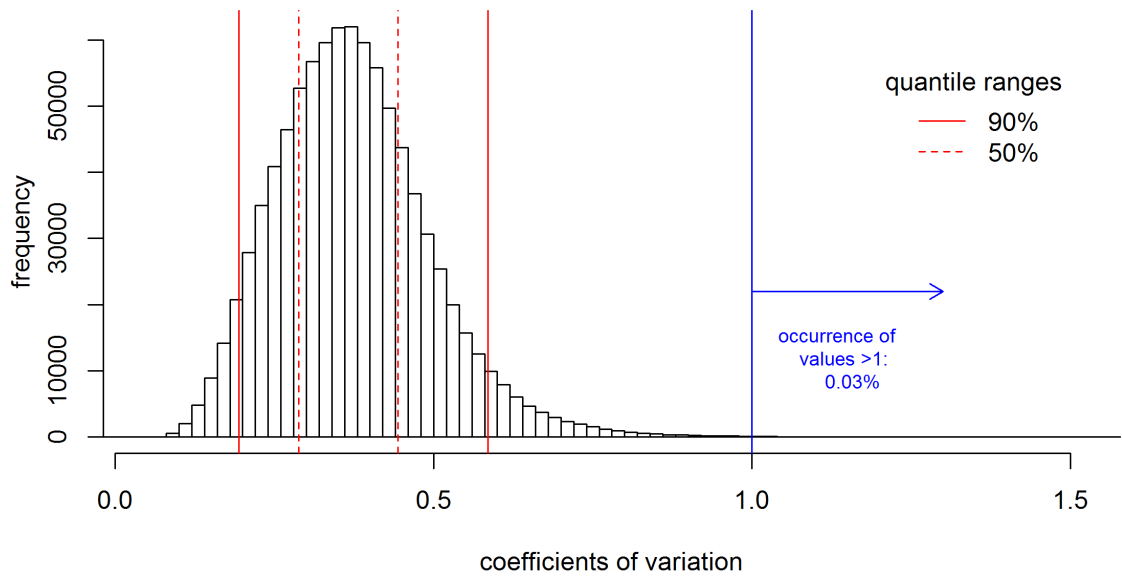
1
2
3
4
5

Figure-5 continued: This is repeated for all image pixels (except for boundary pixels) resulting in the leftmost picture.



1
2
3
4
5

Figure 5 continued: Subfigures (b)-(e) illustrate the procedure from dataset (b, left) to the environment measures (c-e, left), to the coefficients of variation for different environments (c-e, right) and to the final describing average pattern (b, right).

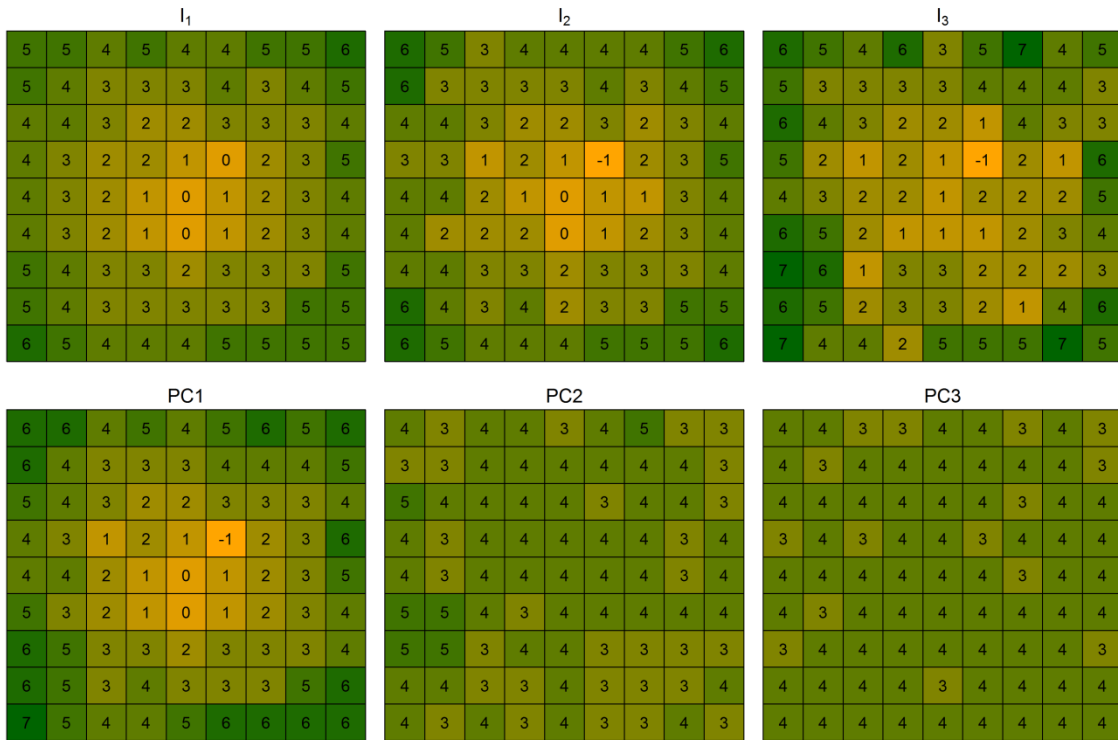


1

2

3 Figure 6: Coefficient of variation for the **ASTERLST** time series data. The median coefficient
 4 of variation is 0.34, the mean value 0.35. 90% of the calculated values are within the range of
 5 0.19 and 0.55 (red lines), 50% within the range of 0.27 and 0.42 (red dashes); 0.03% of the
 6 values are larger than 1 (blue arrow).

7

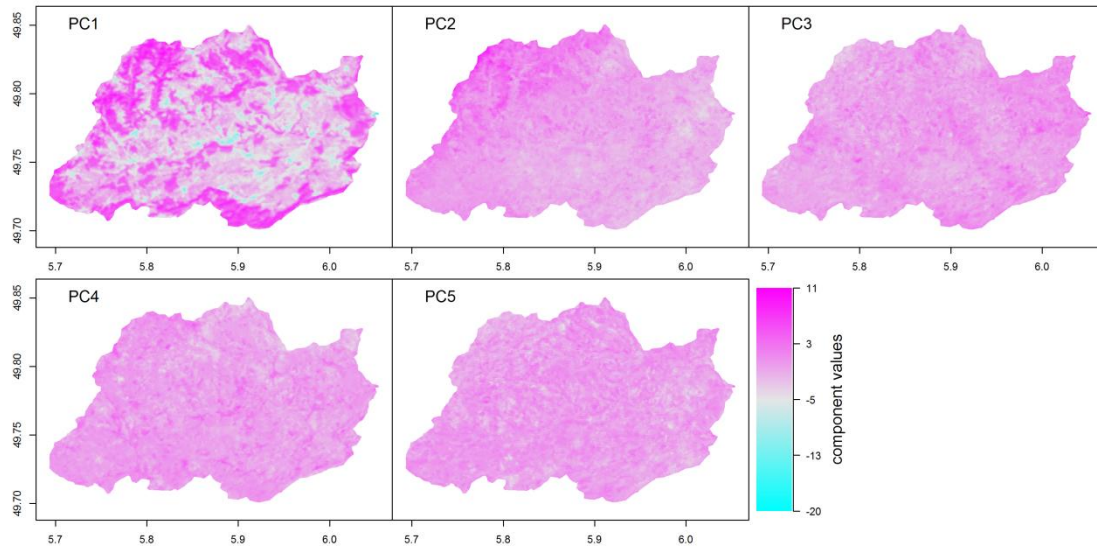


1

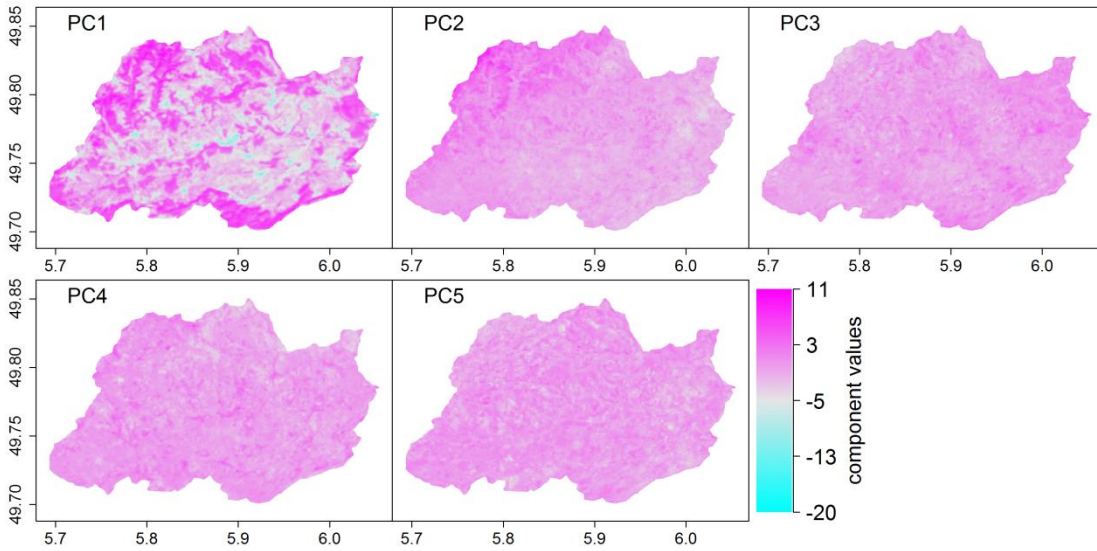
2

3 Figure 7: Principle component analysis for a designed dataset. The data are the same as for
 4 Fig. 5. The first row shows the pattern of the original data (I_1 - I_3), the second row shows the
 5 three resulting principle components (PC1-PC3). The PCs are scaled to the same numeric
 6 domain as the original data and colored alike (orange for low, green for high values). PC1
 7 shows the dominance of the concentric pattern explaining 90.5% of overall variance of the
 8 data. PC2 and PC3 are more homogeneous and describe the noise of the construction of the
 9 dataset.

10



1



2

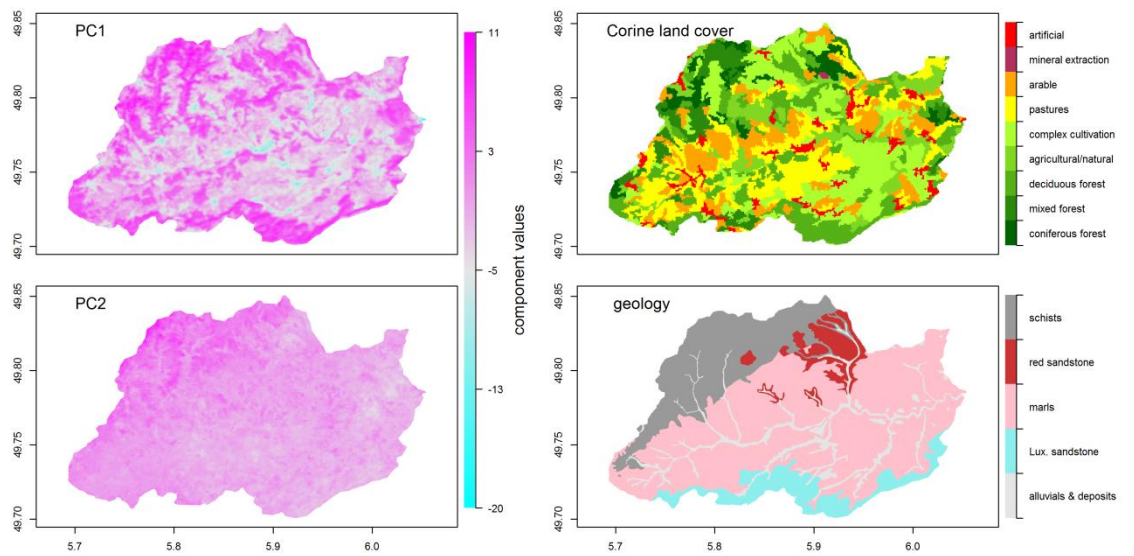
3

4

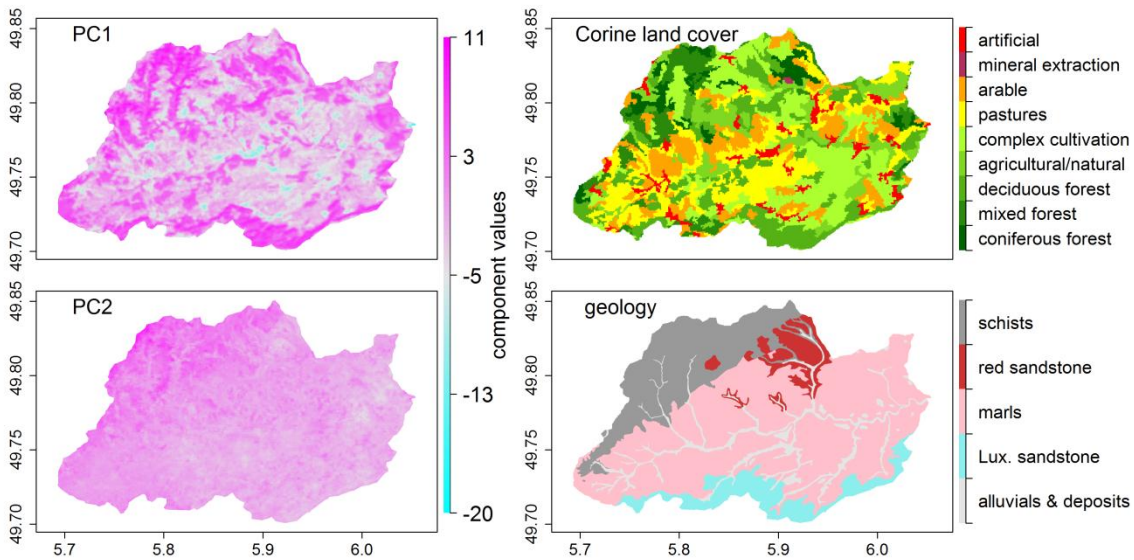
Figure 8: The first 5 components of the PCA for the LST time series data.

5

1



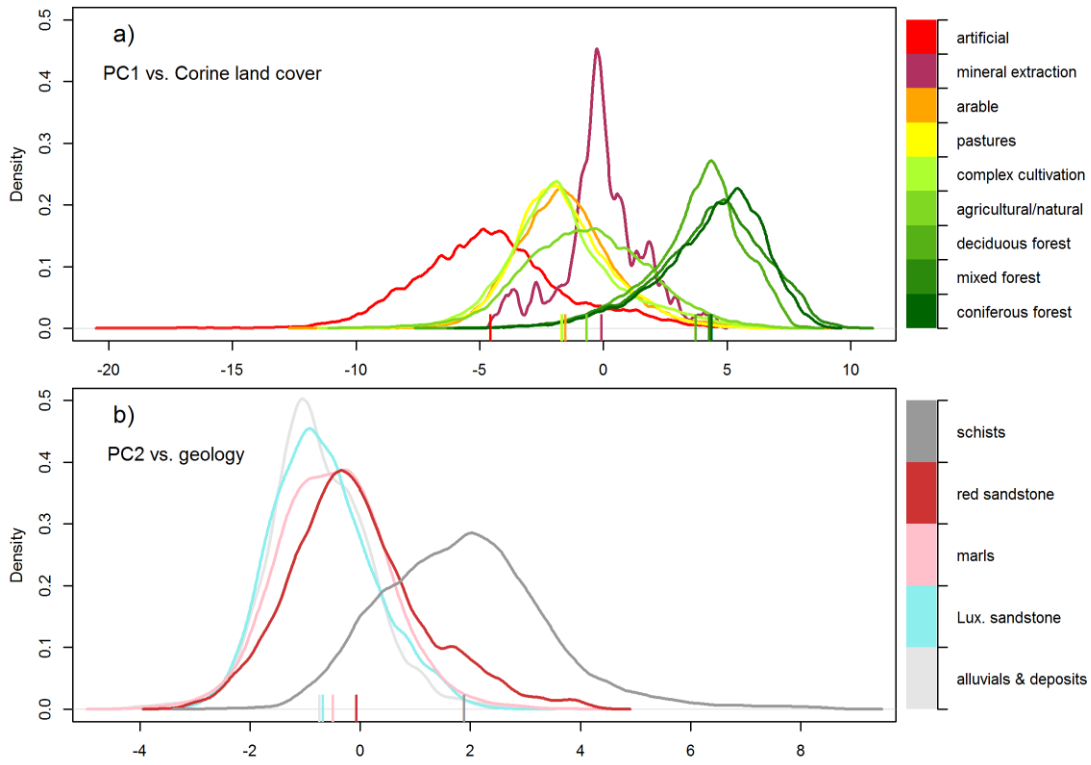
2



3

4 Figure 9: The first and second component of the PCA for the LST time series data (left) next
5 to the patterns of the illustration of Corine land cover and geology data (right) of the Attert
6 catchment.

7



1
2
3
4
5
6
7

Figure 10: Comparison of component values and spatial information for the Attert catchment. The density distribution of the component values (PC1 in a; PC2 in b) are shown for the different classes of the spatial datasets (Corine land cover in a; geology in b). Mean values of the distributions are shown as vertical bars at the bottom line.

1
2
3
4
5
6
7
8
9

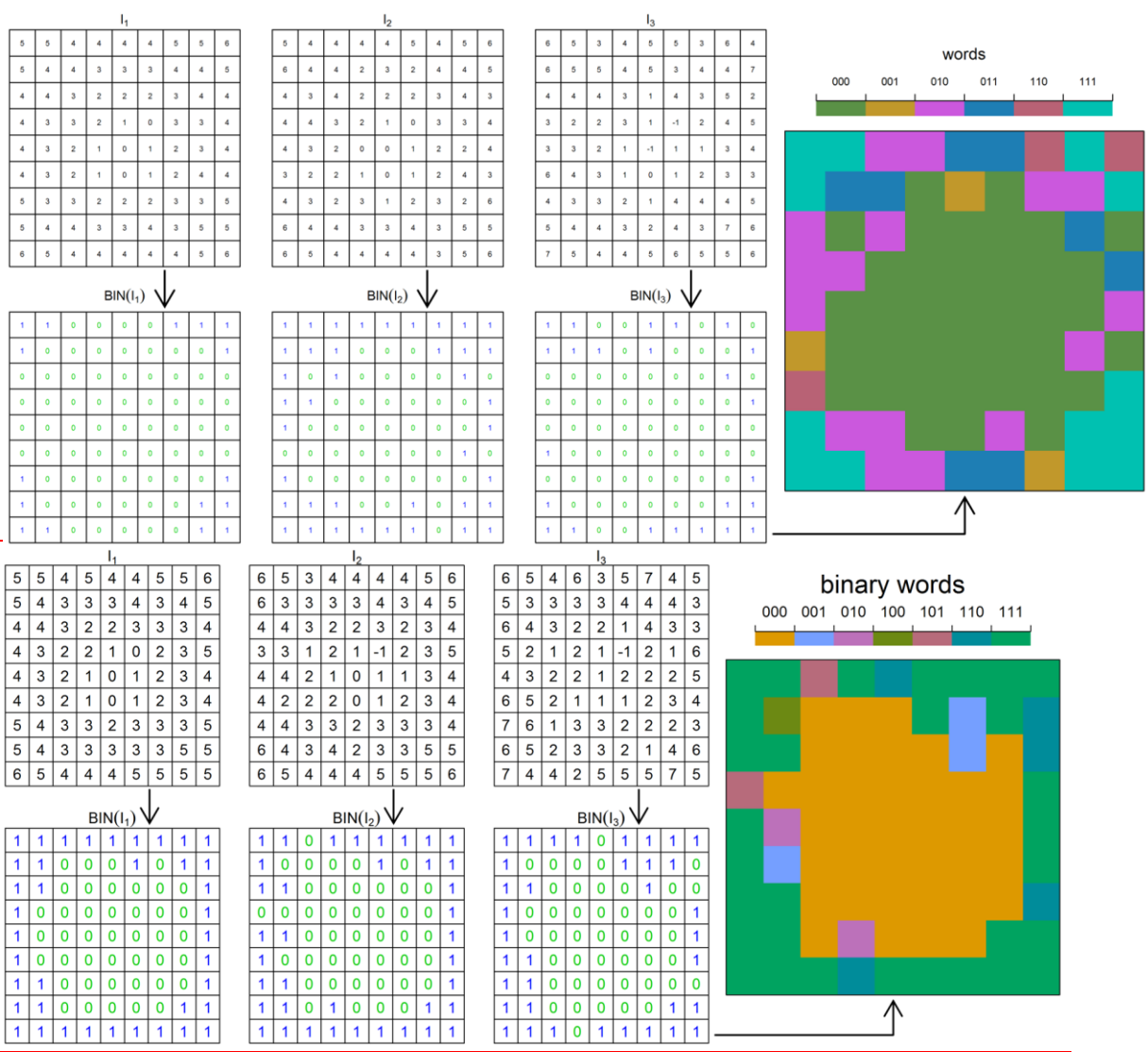
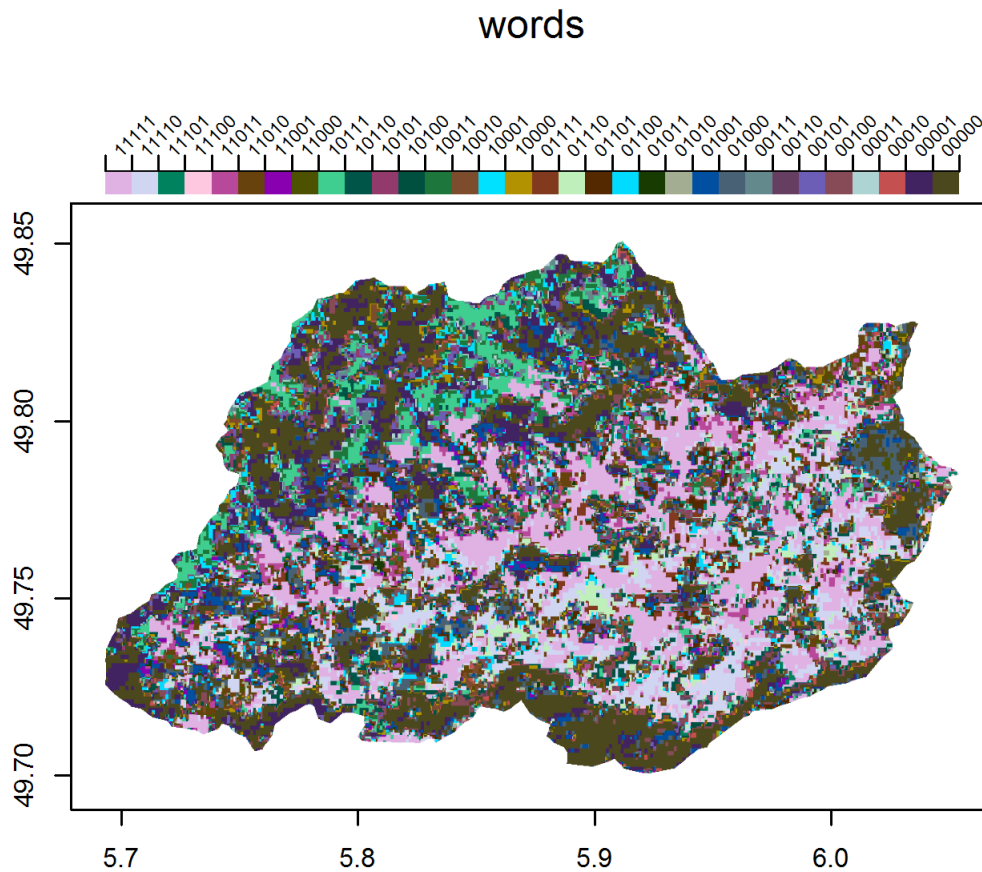


Figure 11: Construction of “binary word” classification for a designed dataset. The data are the same as for Fig. 5. On the left, the three images are binarized (BIN) from the upper to the lower panel. Values larger than the median are converted to 1 (blue), values lower are converted to 0 (green). The right panel shows the aggregated words for the three datasets. Not every possible occurrence of words is produced (maximum: $2^3=8$).



1

2

3 Figure 12: Behavioral classification of the subset LST time series data. The algorithm is
 4 producing $2^5=32$ classes of different frequency. The image shows the full bandwidth with
 5 classes named in the legend.